A Study of the Effect of Various Material Combinations on the Bolted Contacts of Busbars

by

James Gatherer

A thesis submitted to the Graduate Faculty of
Auburn University
in partial fulfillment of the
requirements for the Degree of
Master of Science

Auburn, Alabama
August 3, 2013

Keywords: busbars, electrical contact, bolted joint

Approved by

Robert L. Jackson, Chair, Associate Professor of Mechanical Engineering
Song-yul Choe, Professor of Mechanical Engineering
George T. Flowers, Professor of Mechanical Engineering

Abstract

The reliability of bolted joints is a concern for high-powered devices as the generated heat and thermal expansion could loosen the connections over many actuation cycles. There currently appears to be relatively little information on what material combinations, surface finish, etc. would be beneficial. This work experimentally evaluates the reliability of bolted contacts over 100 cycles and develops theoretical models to predict the relative bolted contact performance. The experimental test arrangement includes eight busbar pairs connected in series, while a power supply cycles current so that the busbars reach a desired temperature rise. Variations are made to busbar material and thickness, washers, torque, bolt property class, diameter, and head types in 60 different combinations. Each combination is tested three times, and then the cases are compared to each other using statistical methods. As expected, the electrical and thermal cycling fatigues the bolts, and in some cases the limitations of the joint were exceeded.

Statistical analysis was performed on the experimental results, which varied by busbar type. The analysis showed which variables, or combination of variables, were statistically significant in terms of reliability. It was found that roughness, torque and head type were the variables that were statistically significant for the 6 mm copper busbars. The roughness and nut material were statistically significant for 1 mm copper busbars. Last, the roughness, torque, and presence of a Belleville washer were statistically significant.

Acknowledgments

I would like to thank my advisor Dr. Robert Jackson, for his support and encouragement throughout the project, for which I am extremely grateful. In addition, I would like to thank my committee members Dr. Song-yul Choe, and Dr. George Flowers for their help and support.

I would also like to thank Hamed Ghaednia, Hyeon Lee, Amir Rostami and Miles Ulm for all of their help, support and insight through our experiences in the lab and through our conversations.

Additionally I would like to thank my supportive partner Meagan Silas for always being understanding and encouraging. I am thankful for the experiences we have shared since I began graduate school.

Finally I would like to thank my parents Jim and Midge for always being there for me, their encouragement and for always supporting me in my collegiate goals. I would also like to my sister Amy for all of her support while we were both students at Auburn University.

Table of Contents

List of Tables

List of Figures

Chapter 1

Introduction

The use of overlapping bolted joints for conducting electricity has been a popular design choice for many years. Overlapping bolted joints are an excellent choice for conducting power because they are dependable, economical, and versatile [1]. The most common method of joining (aluminum) connections currently is bolting. The joint is easily made with hand tools, steel bolts, and steel washers. However there are questions concerning joint reliability due to the use of dissimilar metals [2]. The study of bolted joints began in 1913, with F.W. Harris [3]. He noted that the drop in voltage between two members, and thus resistance, was a typical way to measure efficiency of equipment. He studied the effects of pressure, current, voltage drop, material combinations, area of contact, and surface conditions. Harris said there was no more universally involved or fundamental set of truths than those involving the transmission of current between bodies. It is required for all machinery. Thus, the electrical losses should be considered during the design process [3].

Holm [4] later established that surfaces in contact are not perfectly flat, but contain numerous minute valleys and peaks known as asperities. Therefore, when two surfaces make contact, current can only flow where the peaks of the surfaces meet. The summation of these conducting areas, or *a-spots*, was found to be much smaller than previously thought, less than 1%. Thus, the roughness of a given surface is of great importance in electrical connections [4].

Therefore, since the main purpose of an electrical connection is to permit continuous flow of current across the contact, it is imperative that good metal-to-metal contact is formed [5]. After reviewing literature, the author [5] concluded that the opposing phenomena of differential thermal expansion, formation of intermetallic compounds, fretting, galvanic corrosion, oxidation,

and stress relaxation may occur [5]. To limit these adverse effects, again after reviewing literature, the author [5] concluded methods such as using various mechanical contact devices, surface preparation, coatings, and lubricants have been used to different degrees of achievement. In addition variations in torque and roughening of the contact surface have been studied.

However, relatively little research has been conducted regarding material combinations of components and their relative significance in joint reliability. Therefore, the individual and group effects of the following combinations will be studied, tested, and statistically analyzed. The first variable analyzed was steel class. Steel class refers to the type of steel used in the bolt and nut of the joint; it is important that the fastener remain strong enough to hold the busbars together under current cycling.   The second variable evaluated was head type. Head type refers to the shape of the bolt, and can include a hex shaped or flange shaped head; this variable can affect outcomes since flange shaped heads possess a larger apparent area of contact between the bolt head and busbar. The third variable seen is the washer. The head type and washer affect the pressure distribution that the fastener exerts on the busbars; thus, the presence of a Belleville washer between the nut and busbar was tested. The fourth variable considered was applied torque, since torque is based off the yield strength of the fasteners and is important in maintaining strong joint contact. The final predictor variable used was roughness, the values of which were calculated from profilometer readings.

1. Organization of Thesis

Chapter 2 of the thesis is a comprehensive background on bolted joints. It includes experimental and theoretical analysis, and includes analysis for copper and aluminum busbars.

Chapter 3 shows the methodology used for the experiments. It explains the test matrix, experiment design, test stand equipment, and results.

Chapter 4 includes a statistical analysis from the tests. It is broken up into three sections. The first section is analysis of the 6mm copper busbars. The second section is analysis of the 1mm copper busbars. The third section is the statistical analysis of the 6mm aluminum busbars.

Chapter 5 is the summary of results from the tests and any conclusions that might be made. It also includes any possible future work that may be done.

Chapter 2

Literature Review

2.1   Introduction

One design option for power transmission is the use of overlapped busbars that have been bolted together.   Overlapping bolted joints are dependable, economical, and versatile, [1] which makes them a good design choice. In addition they deteriorate very slowly, and can operate for decades [6].

A busbar is a form of electrical connector commonly composed of copper or aluminum. Holm said, "The term electric contact means a releasable junction between two conductors which is apt to carry current." [4] Thus, the pieces in contact are known as *contact members*, or *contacts*, and the force that presses the contacts together is known as the contact *load* [4].

Holm [4] established that surfaces in contact are not perfectly smooth. The material in contact deforms, plastically or elastically, upon the application of pressure. Therefore, the points (or asperities) initially in contact grow into contact areas. The total of all these areas is known as the *load-bearing contact area, A_b*. This total is much smaller than the *apparent contact area, A_a* [4]. The apparent contact area is the total area of overlap between two contact members.

2.2   Effect of Current Through Contact

The current becomes constricted at the contact because it can only flow through the small conducting areas of contact where the two surfaces make contact, as seen in Figure 2.1 below. The electrical resistance that results is termed *constriction resistance, R_c*. However *contact resistance, R*, is also observed (it is often used to describe R_i), though it is used regardless there is only constriction resistance or whether a resistance due to film also occurs.   The material

deforms at the actual points of contact, but since the localized pressure is different at the various points, some spots deform elastically, while others may deform plastically [4].

Figure 2.1: Asperity contacts

These load-bearing areas can be separated into three different categories based on the level of current flow, as seen in Figure 2.2. First, there are the segments that make metallic contact. In these areas current flows with very little transition resistance at the boundary, such as when current flows through various crystallites in solid metal. These are known as *a-spots* [4].

Second, there are the segments in which a thin film covers the area of contact. However, this film is thin enough that current can flow regardless of the film type. Common examples of this phenomenon are oxide layers that form on a metallic surface when it is exposed to air [4].

Third, there are the area segments with multi-molecular alien films; these films act as insulators for the contacts. Examples of these types of insulators include tarnish films, such as sulphides and oxides [4].

EXPECTED CONTACT AREA
ACTUAL CONTACT AREA
LOAD-BEARING AREA
QUASI-METALLIC CONTACT AREA
CONDUCTING CONTACT AREA (a-spots)
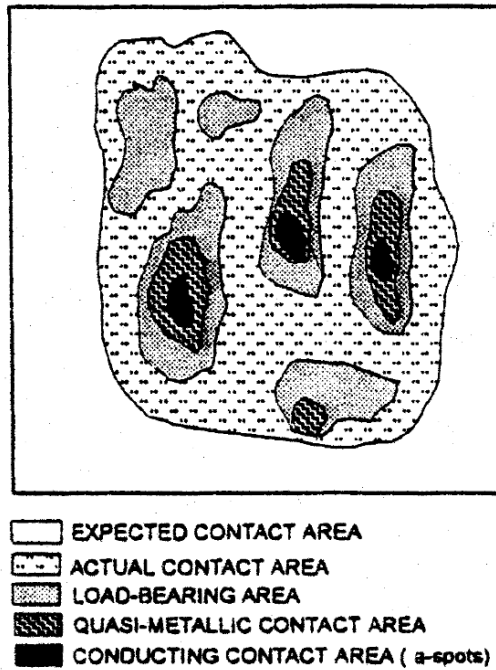
Figure 2.2: Contact area [1] © 2002 IEEE

Holm mathematically showed that the restriction resistance for clean, circular contacts is:

$$R_c = \frac{\rho}{2a} \tag{1}$$

where R is the constriction resistance, a is the radius of the circular contact area, and ρ is the resistivity [4]. However, if a film has formed in the contact, then the film resistance, R_f, must be taken into account. In many real-world applications, the influence of these films on the total contact resistance is insignificant. This is because the rupture of surface films typically forms the contact spots [1]. The equation for R_f is below, where A is the contact area and σ is the resistance over 1 cm² of the corresponding film [4].

$$R_f = \frac{\sigma}{A} \tag{2}$$

6

The contact resistance between flat, prepared metal surfaces is dependent upon many factors. These factors include the area of the surface in contact, the pressure applied, and how the surfaces were prepared. As Melsom and Booth [7] noted, the assumption that the contact between two surfaces consists of only three points is incorrect. If this assumption were true, one could conclude that a constant total pressure would lead to contact resistance being independent of the contact area. However, experiments of aluminum and copper bars clamped together showed that contact resistance was (almost) inversely proportional to the area, suggesting that the pressure per unit area was constant [7].

Under extremely small pressures, the three-point contact theory would likely apply. However, once any significant pressure was applied, deformation of the surface would occur and other points come into contact. This deformation could take the form of flowing, or straining of the material. Inspection of the metal in this study suggested probable instances of significant deformation, thus showing that the three-point contact theory would not apply [7].

Contact resistance is related to the film of air thickness in between the surfaces. While the thickness is small, a small variation could have a large effect on the contact resistance. It is assumed in the paper by Melsom and Booth that "the resistance between two surfaces is inversely proportional to the area when the pressure per unit area is the same, may not be absolutely correct, but it appears more nearly to represent the facts" [7] © 2011 IEEE. Bailey [8] also noted the effect of roughness, and that repeatedly pressing surfaces together without re-roughening would affect the results due to the flattening of asperities, and altering the size and number of a-spots [8]. Naybour later noted on aluminum contacts with a load of 1700 N that the resistance of a newly prepared smooth surface (c.l.a. = 0.06 μm ± 0.02 μm) could be at least 100 times as high than a newly prepared rough surface (c.l.a. = 2.5 μm ± 0.2 μm) using experimental

results [9]. However, testing an aluminum-aluminum joint showed that a smooth surface joined with a rough surface would result in the electrical resistance not increasing with time [9].

2.2.1   Bolted Joint Design

Braunovic, for a project in sub-station mechanisms, noted that the most important design parameters necessary to guarantee connector reliability were electrical efficiency, mechanical strength, ease of installation, and corrosion resistance [1]. The connector electrical efficiency is largely dependent on the contact joint resistance. This contact joint resistance is determined by the distribution of conducting spots and contact area; these are a function of the applied force, method of which the force is applied and surface finish [1]. Sufficient mechanical strength is also needed in order to preserve the mechanical integrity of the connector, which will allow the connector to withstand the applied loads, such as expansion and contraction strains due to thermal and electrical load cycling [1]. In addition, ease of installation is important for economic reasons, but is outside the scope of this work. Finally, a connector should be able to withstand the effects of the environment; therefore, it should have good corrosion resistance. This is especially true for aluminum [1].

In Bailey's research, it was found that keeping the surfaces flat, removing burs, good alignment, accurate hole drilling, and not over-tightening of the bolts (and thus distorting the flat surface) were desirable [8]. Bailey also observed that factors leading to poor performance included insufficient surface preparation, the use of small bolts, too small of a contact area, and a poor joint design that allowed loosening. Tightening the bolts evenly was also found to be important to performance. Thus, Bailey recommended that an area of contact be approximately

8

ten times the thickness of the bar and have a pressure of 1500 to 1750 psi (10.3 - 12.1 MPa) to achieve good performance [8].

Aluminum-to-aluminum joints with the lowest initial contact resistance proved to be the most stable throughout the entire test, while joints with higher initial contact resistance failed in the first couple of cycles [10]. A relatively slight reduction in initial resistance was found to have a significant increase in part life [6]. In addition, surface preparation was shown to be important [11], as metal-metal adhesion is needed to achieve joints with low-resistance.

It is self-evident that using nuts and bolts with greater yield strength and diameters can enlarge contact loads [8]. Bailey showed that large bolts with a level bolt load distribution and highly rigid clamps attained stable joints, and a stronger fastener led to a larger contact area. Therefore high-tensile steel bolts may be recommended in order to generate adequate pressure [8].

In many cases, the load is distributed in such a way that the pressures required to produce a-spots are developed only in the area directly underneath the bolt head [8]. If a larger bolt size is used, then this area will increase quickly [5]. Higher pressures over a larger area will generate more a-spots, and therefore lower resistance. The pressure distribution can also be improved through the use of clamping plates, which are preferred to washers. For small bars, clamping plates with external bolts may be more efficient than through bolts [8].

Braunovic showed that an increase in contact force relates to a decrease on contact resistance [12]. He displayed the well-known dependence of contact resistance, R_c, on contact force, F_c, with the relationship

$$R_c = aF_c n \qquad (3)$$

where *n* and *a* are dependent on the bars' surface finish [12]. One of the most important parameters to ensure high connector performance is for the real contact area to be adequately large. This will ensure the presence of spare contact spots, despite initial and long-term deterioration [1].

New designs are been tested [13] which result in an increase of contact pressure and penetration compared with classical designs. These new designs show improved reliability of the electrical connection [13].

2.2.2   Contact Force

Schoft et al. [14] noted that it was necessary to study the relation in joint resistance and force, in addition to joint force and time, conditional on initial force and temperature. When creep deformation of the busbars occurs, the joint force lessens. This causes the number and area of the a-spots to decrease, which causes the constriction resistance to occur [15]. Hence, the decrease of joint force was assumed to be critical in increasing resistance and eventually failure [14]. Zhou also found contact force (due to initial tightening) to be critical to keep the parts from overheating, in his research on loose connections [16].

Schoft et al. [15, 17] noted different relations between joint force and other parameters. First, the reduction of force increases with the rising joint temperature [18]. Second, the reduction of joint force, following tightening, in joints will happen quicker, the more inhomogeneous the initial stress distribution is [18]. Lastly, the (long-term) performance of the joint force depends on the material properties, temperature of the busbars and mechanical stress in the joints [17, 18].

In addition, Schlegel et al. [19] studied the relation of resistance and force on copper-copper busbar joints. The decrease of joint force over time was observed, and the minimum joint force needed was found to be 20% of the initial force. Otherwise the joint resistance will grow. In addition, different material combinations were tested while joint resistance and force were monitored. Two copper materials with different degrees of cold work were used. In addition, washers were compared with spring washers. Each of these (four) combinations were tested at 105°C, 140°C and 160°C. It was found that the material with greater initial mechanical properties showed worse long-term behavior in terms of force reduction. Therefore, members that are less cold worked should be chosen because they gave higher strengths. Last, it was found that force reduction becomes critical at temperatures equal and greater to 140°C [19].

2.2.3 A-Spots

Schoft et al. [17] used experimental work and FEM to study a-spots. The experiment consisted of a quasi-rigid rack that held a heatable rod, force gauge and two busbars bolted together. During an experiment, the rod is heated. However the rack hampers the rod's thermal expansion, and forces the joint force to increase. Once the joint force hits 1.5 kN, a current of 800 A was applied. Once the joint hit 25 kN, the heating rod turned off. Throughout tightening the resistance decreased as the joint force increased. During releasing and cooling there was a small increase in resistance [17]. A similar experiment was used in [14].

The conclusion from the work by Schoft et. Al [15, 17] found that the joint resistance during tightening and releasing exhibits characteristic hysteresis as shown in Figure 2.3. Second, it was found that as the joint force increases, the number of a-spots increases gradually. However, the mean radius of the a-spots increases until some constant level. Third, during

11

releasing, there is a decrease in the number of a-spots. However, some plastically deformed areas remain in contact when the joint force is zero. During release the mean radius of the a-spots is approximately independent of the joint force; this was determined using FEM [15, 17]. After the experiment in [14] the busbars remain stuck together without any outside force.
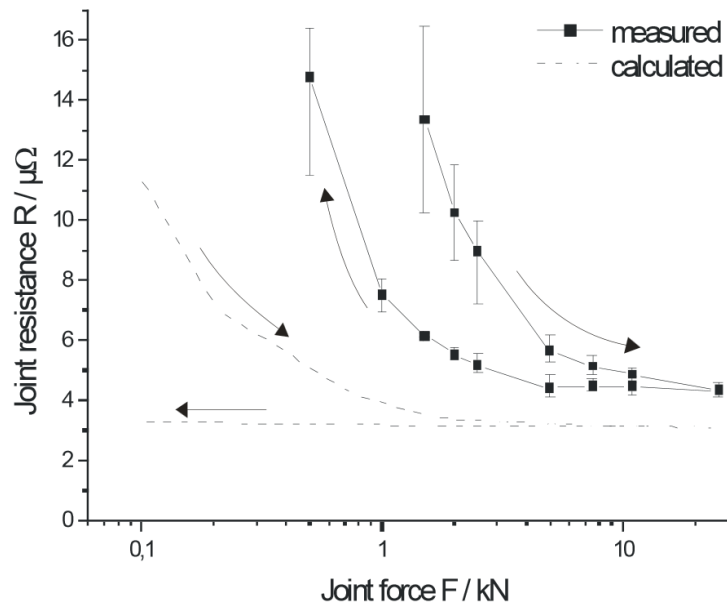
Figure 2.3: Joint resistance versus force for brushed and machined busbar joints [17] © 2002 IEEE

Naybour noted that if one of the contact members is plastically deformed it would create a low-resistance contact. Therefore, combining a soft and hard member can result in a joint with low contact resistance [9].

2.2.4   Chemical Reactions

Another cause of joint aging is chemical reactions on the constriction areas. The speed with which chemical reactions take place is dependent on the temperature. In aluminum-

aluminum contacts, electrical current and ambient temperature has a significant effect on the lifetime of the bolted joint [6, 20]. Zhou, in his research on loose joints, also found current to be critical in preventing the joint from overheating [16].

2.2.5   Busbar Overlap

Melsom and Booth [7] studied the effect of the length of the overlap between busbars. If the span of overlap length, l, is much greater than the bar thickness, t, then the resistance of the overlapping section will be close to that in which two conductors are in parallel. However, when the overlap is significantly reduced, then this is no longer true due to the distortion of the streamlines of the electrical current. The distortion is dependent only upon the ratio between the overlap and the thickness of the bar. Assuming the two bars have the same width, the width will not have any effect on the flow of current [7]. This also assumes the bars are sufficiently wide; otherwise there would be an increase in the resistance.

Melsom and Booth [7] carried out an experiment in which current was passed through tinfoil, and the subsequent voltage drop measurements were taken over tinfoil that represented different amounts of overlap in bolted busbars. Different ratios of busbar overlap length, l, and thickness, t, were tests to determine the effect of the ratio l/t on resistance, specifically resistance due to stream-line distortion. It was found experimentally that the ratio l/t had a relatively large effect on resistance when the ratio was less than 3. However, l/t values greater than four had relatively little difference in relation to resistance [7].

2.2.5   Plating

Films can develop on material surfaces, which can lead to a buildup in electrical resistance. One way to combat this is to plate the surface. Plating prevents corrosion and improves the joint stability. The most commonly used materials are nickel, cadmium, silver, and tin. Farahat et. al [21] performed a current cycling test and placed the joints in humid and dry environments. It was concluded that silver and nickel were excellent plating materials, but nickel was the most practical due to its relative cost [21, 22].

However plating can be porous, which leaves the surface vulnerable to trapped contaminants. In addition to simple plating, a corrosion inhibitor compound can be used or the thickness could be increased. Or, both methods could be used [23]. Jackson showed that nickel plated to copper is also advantageous and showed good joint stability [24]. In addition, for copper-aluminum joints, Braunovic noted that nickel-coating connections under various operating and environmental conditions boosted the joint stability [5].

Braunovic [25] showed that fretting strongly affects nicked-coated aluminum wire connections. Nickel's low strength can hurt its ability to protect aluminum conductors from fretting. The coating wears out due to changes in resistance, and oxide layers and fretting wear debris builds up in the contact area. This layer interferes with the flow of current. The use of a lubricant, using low slip amplitudes and using high contact loads are ways to improve reliability [25]. Additionally, other methods of improving joints is through the use of a grease or jelly [26], however that is outside the scope of this work.

2.2.6 Computer Modeling

In addition, many studies use computer modeling to analyze connector performance. Popa and Dolan created a 2D and 3D finite element model to discover the optimal geometry for

contacts. The results show a concentration of heat and magnetic flux to be in the center of the

contact [27], as shown in Figure 2.4 and Figure 2.5.
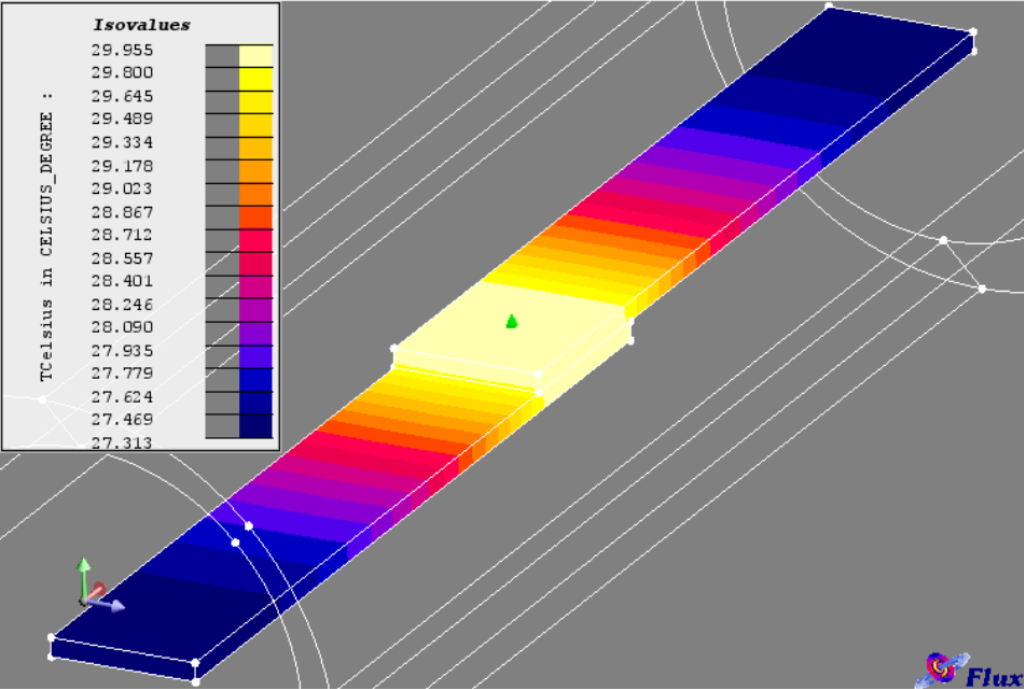
Figure 2.4: Temperature distribution of busbar pair [27]
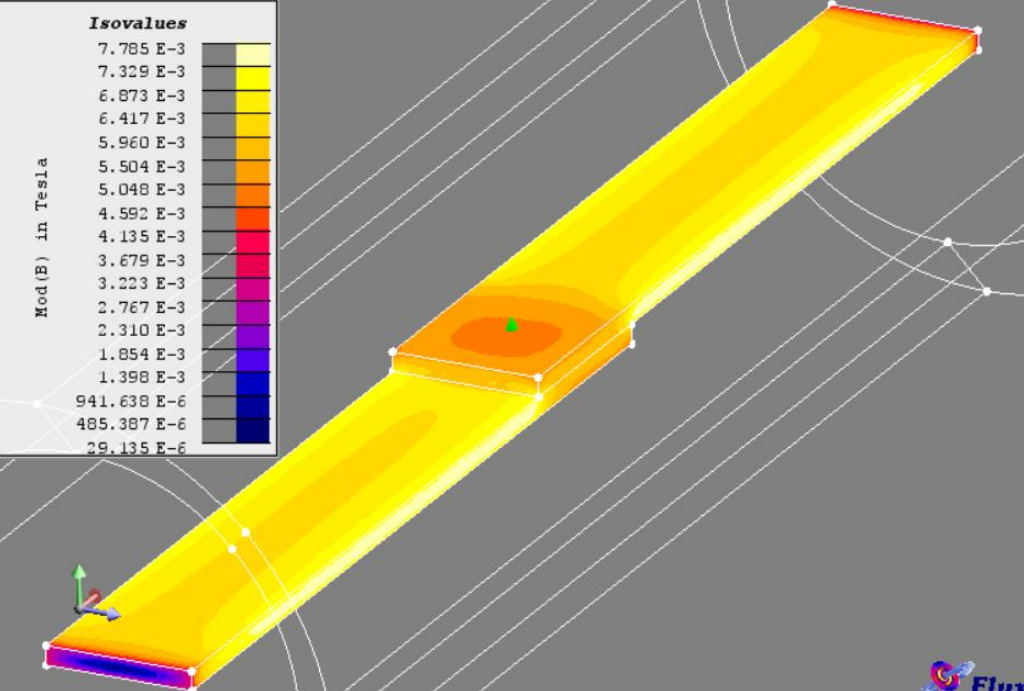
Figure 2.5: Magnetic flux density distribution of busbar pair [27]

In addition, Wileman et al. [28] performed FEA to determine the stiffness of members in bolted joints. The equation below was used, where k_m is the combined stiffness of the two members, E_b is the elastic modulus of the bolt, d is the diameter of the bolt clearance hole, L is the grip length, and A and B are constants found in Table 2.1.

$$\frac{k_m}{E_d} = Ae^{B(\frac{d}{L})}$$
(5)

In addition the results disproved the cone model for member stiffness as seen in [29].

Table 2.1: Stiffness considerations [28] © 1990 IEEE

Material	Poisson Ratio	Elastic Modulus (GPa)	A	B
Steel	0.291	206.8	0.78715	0.62873
Aluminum	0.334	71.0	0.79670	0.63816
Copper	0.326	118.6	0.79568	0.63553
Gray Cast Iron	0.211	100.0	0.77871	0.61616

2.3   Effect of Current Cycling

When current flows between surfaces it usually only flows through points of contact, known as a-spots. The parts heat up due to the phenomenon of Joule Heating. This causes the shape to change due to thermal expansion and softening, which causes mechanical loads to act upon the surface. Upon the shape of the surface changing, the contact area (and thus contact resistance) will also change. Therefore it becomes a loop of the mechanical forces, area of

contact, electrical resistance, current field, temperature gradient, material properties, and then mechanical forces fluctuating and affecting the other properties [30]. This is shown in Figure 2.6.
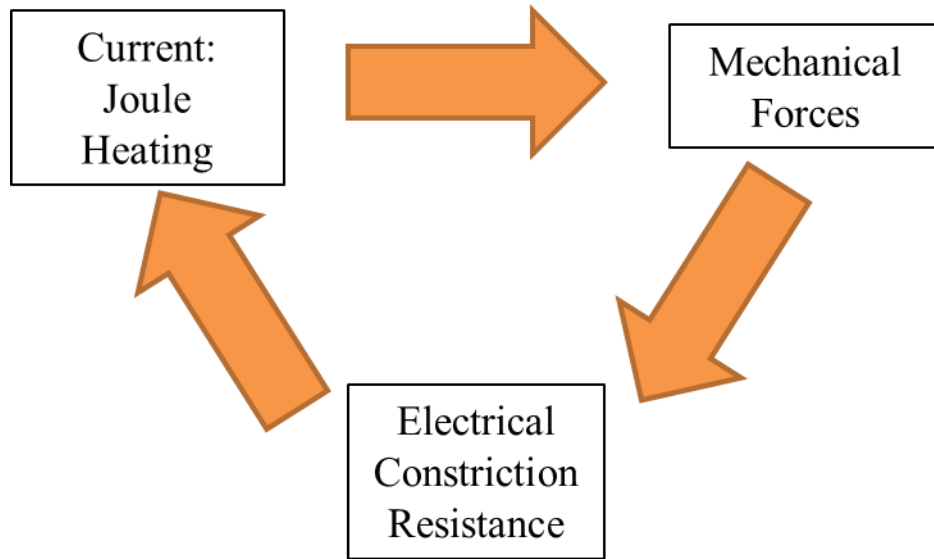
Figure 2.6: The effect coupling electrical, thermal and mechanical behavior on a bolted joint

In order to accurately model a contact, a complete model including electrical, thermal, rough surface contact and mechanical models needs to be formed. Below are the equations or elasticity (in cylindrical coordinates) [30]. The radial-direction strain, ε, and shear strain,γ, are functions of the elastic modulus, E, Poisson's ratio, υ, normal stress, σ, shear stress, τ, change in Temperature, ΔT, and the coefficient of thermal expansion, α.

$$\varepsilon_r = \frac{1}{E}[\sigma_r - \nu(\sigma_\vartheta + \sigma_z)] + \alpha\Delta T \tag{6}$$

$$\varepsilon_\vartheta = \frac{1}{E}[\sigma_\vartheta - \nu(\sigma_r + \sigma_z)] + \alpha\Delta T \tag{7}$$

$$\varepsilon_z = \frac{1}{E}[\sigma_z - \nu(\sigma_r + \sigma_\vartheta)] + \alpha\Delta T \tag{8}$$

17

$$\gamma_{r\vartheta} = \frac{2(1+v)}{E}\tau_{r\vartheta} \tag{9}$$

$$\gamma_{rz} = \frac{2(1+v)}{E}\tau_{rz} \tag{10}$$

$$\gamma_{\vartheta z} = \frac{2(1+v)}{E}\tau_{\vartheta z} \tag{11}$$

Below is the Electrical Field Equation. Current, I, is dependent upon the gradient of the electric potential field, Φ, and electrical conductivity, σ [30].

$$I = \sigma\nabla\varphi \tag{12}$$

Below is Fourier's law, where the total heat, Q, which incorporates Joule Heating. The total heat is dependent upon the gradient of the temperature field, T, and thermal conductivity, k.

$$Q = k\nabla T \tag{13}$$

Below is the equation of heat due to Joule Heating, which is calculated using current, I, and electrical resistivity, ρ [30].

$$Q_{joule} = I^2\rho \tag{14}$$

Based on equations 6-14, when electrical current flows through a contact, the temperature and stresses rise, eventually causing it to yield. However, if the part cools, then a reduction in contact force causes some of the contact spots to rupture. If current flows again, these contact spots may not reform, due to insufficient pressure needed to close the gaps. In addition, load relaxation enables fretting and oxidation in the contact. Conducting debris will form, which aids the metallic contact; however, additional current cycling will reduce the metal-metal contact, and oxides will form layers at the contact. This will increase the contact resistance and thus the temperature. The temperature can continue to rise to the point of joint failure. Therefore a key cause of initial contact deterioration is stress relaxation [12].

Braunovic [12] demonstrated the importance of this concept when relaxation occurred during testing, yet the temperature and resistance were unresponsive. Also, the largest changes

in contact force occurred during cooling, showing that cooling is more damaging than heating. The changes in temperature, force, and resistance initially increased after the test began, but approached steady state after approximately 40 heat cycles. Thus, greater stress relaxation occurred, since the higher the force used to tighten the joints, the greater the stress was produced from the current [12]. The tightening and thermal expansions superimpose and combined to cause high stress.

Heat cycling has a large effect on the contact load, as seen in the relatively large loss of contact load during cooling. Changes could also be seen in contact resistance, but they were much smaller. The temperature showed no significant changes in this heat cycling experiment [12]. Braunovic said that current-cycling tests were a good basis for assessing the performance of a joint [10].

2.3.2   Washers

It is important to preserve the mechanical integrity of an electrical joint. Failure to do so could lead to an increase in temperature, which can cause thermoelastic ratcheting, creep, accelerated oxidation, and stress relaxation. In addition it could result in an increase in resistance, which could lead to a decrease in contact force. There are different ways to maintain a satisfactory joint. One method of doing so is to add washers. Previously, this was done using flat lock-spring washers. However, Belleville and transition washers have been adapted [31].

Belleville washers are beneficial because they counteract the variations in force due to the variations in temperature and dissimilarities in the thermal expansion of bolts and busbars [31]. Belleville washers apply some predetermined force to the busbars. When outside forces are applied, they can absorb elastic deformation. Belleville washers store up energy, suspend

load measurements and dissipate shock load due to a high force/deflection ratio. They are beneficial on bolted joints because they counteract loosening that occurs in bolted joints due to creep, stress relaxation and thermal expansion. The Belleville washers are commonly suggested for bolted joints that comprise of aluminum busbars and steel bolts. This is due to aluminum having a significantly higher coefficient of thermal expansion than steel and the resilience of Belleville washers counteracts this [2].

Braunovic showed that Belleville washers, compared to spring lock washers, could improve the performance of bolted joints. Belleville and spring lock washers exhibited similar performance levels in terms of the resistance-force association when the current cycled was consistent, but when the current was increased, the Belleville washers had a much smaller variation in contact force compared with the spring lock washers [12]. However later Braunovic showed that under current cycling the Belleville washer combined with thick flat washers resulted in a reasonably mechanically stable joint [10].

2.4   Motivation

While there is much information available on overlapping bolted joints, there is comparatively little information available on the significance of different material parts and their combinations, which affect the reliability of bolted joints. This thesis will analyze the effectiveness of three part combinations: the use of a washer, the shape of the bolt head, and the class of steel of the bolt and nut. In addition, the applied torque and surface roughness will also be taken into account, as these have proven important mitigating variables in previous studies. Data will then undergo statistical analysis to determine which combination of variables is most conducive to improving the reliability of a bolted joint.

Chapter 3

Overlapping Bolted Joints Experiment

An experiment was designed and executed to test the reliability of bolted joints. A bolted joint consists of two busbars and a fastener. A schematic of a busbar is shown in Figure 3.1 and properties are shown in Table 3.1.

Three different types of busbars were tested: 1 mm thick copper busbars, 6 mm thick copper busbars, and 6 mm thick aluminum busbars. It is advantageous to use copper compared with aluminum because of its relatively low electrical resistivity (1.72×10^{-8} Ωm vs. 2.65×10^{-8} Ωm). However copper is more expensive than aluminum. Similarly, thicker busbars will result in lower electrical resistance, but more material increases the cost.
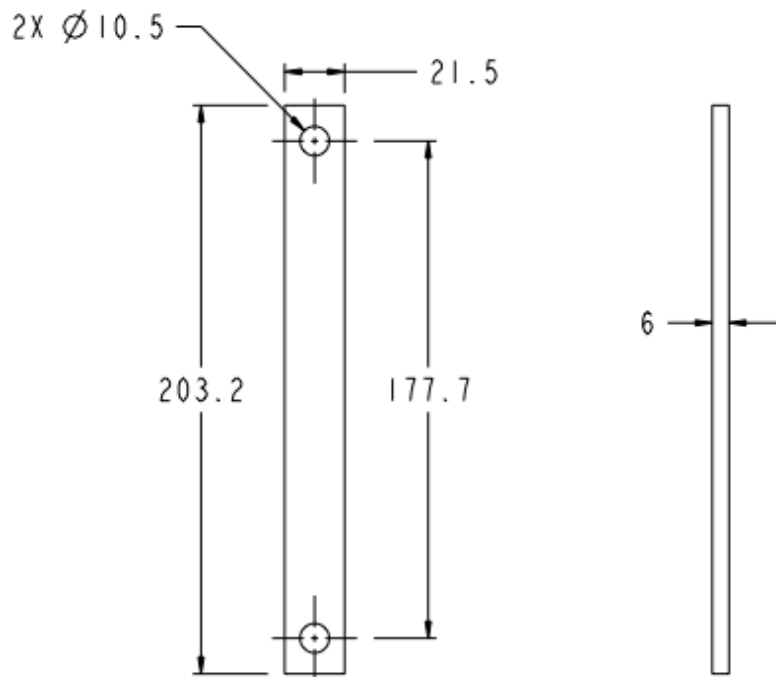
Figure 3.1: Diagram of a single busbar (all values in mm, ±0.25)

Table 3.1: Busbar properties

Copper Busbar Material	C110000 HI Copper
Aluminum Busbar Material	5052 H32 Aluminum
Nickel Plating	ASTM B689-97 2.54-5.08 Microns thick

As seen in Figure 3.2, two busbars were coupled with a single bolt and nut to form a bolted joint. They were torqued using an electronic torque wrench.

Figure 3.2: Single overlapping bolted joint

3.1 Test Variables

In addition to testing busbars of different materials and thicknesses, six material variables were tested: bolt property class, bolt head shape, the presence of a Belleville washer, the initial

applied torque, roughness of the busbar surface, and the material of the nut (1 mm copper busbars only). The specific combinations tested (test matrix) were specified coordinating with the sponsor and are given in the test matrix in Table 3.2. The tables show the 60 different cases that were tested. Cases 21-24 were eliminated from the test after the sponsor decided only four test cases with the pan head type would be tested. The cases near the end (cases 57-64) were considered special cases. The special cases comprised of bolted joints using brass nuts or high torques and were tested last.

Each case in the test matrix was tested three times. The number of times each case was run was decided through coordination with the sponsor. In each full test, the power was cycled 100 times. One cycle included the current being turned on at a constant value for one hour, followed by the power being turned off for one hour. The time intervals during current cycling and current values were determined after running steady-state tests and preliminary tests. The end goal was to achieve a temperature rise of roughly 100°C, or an overall temperature of approximately 125°C. To replicate realistic application conditions, the sponsor desired that the busbars rose to these temperatures. A sample of one cycle from a test is shown in Figure 3.3.
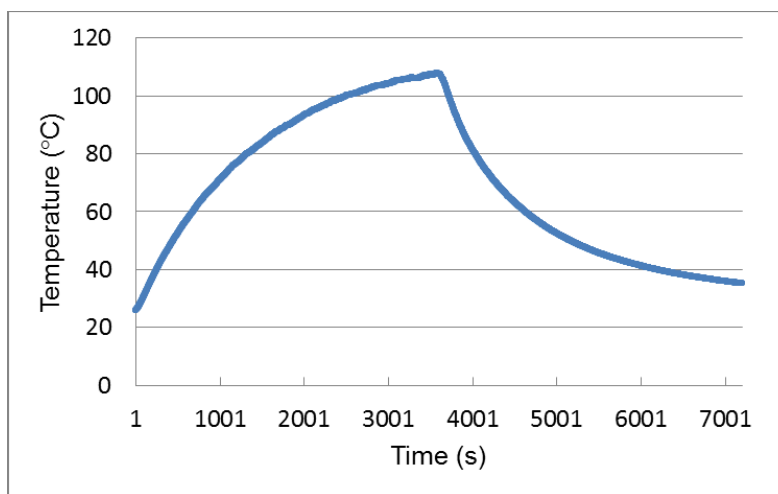

Figure 3.3: Steady state test

23

Table 3.2: Test matrix

Case	Material	Thickness (mm)	Bolt Property Class	Dia/Thread	Bolt Head	Washer type	Torque
1	Cu	1	8.8 (grade 5)	M6 UNC	Hex	None	50% of yield
2	Cu	1	8.8	M6 UNC	Hex	None	75% of yield
3	Cu	1	8.8	M6 UNC	Hex	Crest cup	50% of yield
4	Cu	1	8.8	M6 UNC	Hex	Crest cup	75% of yield
5	Cu	1	8.8	M6 UNC	Flange	None	50% of yield
6	Cu	1	8.8	M6 UNC	Flange	None	75% of yield
7	Cu	1	8.8	M6 UNC	Flange	Crest cup	50% of yield
8	Cu	1	8.8	M6 UNC	Flange	Crest cup	75% of yield
9	Cu	1	4.8	M6 UNC	Pan	None	50% of yield
10	Cu	1	4.8	M6 UNC	Pan	None	75% of yield
11	Cu	1	4.8	M6 UNC	Pan	Crest cup	50% of yield
12	Cu	1	4.8	M6 UNC	Pan	Crest cup	75% of yield
13	Cu	1	10.9 (grade 8)	M6 UNC	Hex	None	50% of yield
14	Cu	1	10.9	M6 UNC	Hex	None	75% of yield
15	Cu	1	10.9	M6 UNC	Hex	Crest cup	50% of yield
16	Cu	1	10.9	M6 UNC	Hex	Crest cup	75% of yield
17	Cu	1	10.9	M6 UNC	Flange	None	50% of yield
18	Cu	1	10.9	M6 UNC	Flange	None	75% of yield
19	Cu	1	10.9	M6 UNC	Flange	Crest cup	50% of yield
20	Cu	1	10.9	M6 UNC	Flange	Crest cup	75% of yield
25	Cu	6	8.8	M10 UNC	Hex	None	50% of yield
26	Cu	6	8.8	M10 UNC	Hex	None	75% of yield
27	Cu	6	8.8	M10 UNC	Hex	Crest cup	50% of yield
28	Cu	6	8.8	M10 UNC	Hex	Crest cup	75% of yield
29	Cu	6	8.8	M10 UNC	Flange	None	50% of yield
30	Cu	6	8.8	M10 UNC	Flange	None	75% of yield
31	Cu	6	8.8	M10 UNC	Flange	Crest cup	50% of yield
32	Cu	6	8.8	M10 UNC	Flange	Crest cup	75% of yield
33	Cu	6	10.9	M10 UNC	Hex	None	50% of yield
34	Cu	6	10.9	M10 UNC	Hex	None	75% of yield
35	Cu	6	10.9	M10 UNC	Hex	Crest cup	50% of yield
36	Cu	6	10.9	M10 UNC	Hex	Crest cup	75% of yield
37	Cu	6	10.9	M10 UNC	Flange	None	50% of yield
38	Cu	6	10.9	M10 UNC	Flange	None	75% of yield
39	Cu	6	10.9	M10 UNC	Flange	Crest cup	50% of yield
40	Cu	6	10.9	M10 UNC	Flange	Crest cup	75% of yield
41	Al	6	8.8	M10 UNC	Hex	None	50% of yield
42	Al	6	8.8	M10 UNC	Hex	None	75% of yield
43	Al	6	8.8	M10 UNC	Hex	Crest cup	50% of yield
44	Al	6	8.8	M10 UNC	Hex	Crest cup	75% of yield
45	Al	6	8.8	M10 UNC	Flange	None	50% of yield
46	Al	6	8.8	M10 UNC	Flange	None	75% of yield
47	Al	6	8.8	M10 UNC	Flange	Crest cup	50% of yield
48	Al	6	8.8	M10 UNC	Flange	Crest cup	75% of yield
49	Al	6	10.9	M10 UNC	Hex	None	50% of yield
50	Al	6	10.9	M10 UNC	Hex	None	75% of yield
51	Al	6	10.9	M10 UNC	Hex	Crest cup	50% of yield
52	Al	6	10.9	M10 UNC	Hex	Crest cup	75% of yield
53	Al	6	10.9	M10 UNC	Flange	None	50% of yield
54	Al	6	10.9	M10 UNC	Flange	None	75% of yield
55	Al	6	10.9	M10 UNC	Flange	Crest cup	50% of yield
56	Al	6	10.9	M10 UNC	Flange	Crest cup	75% of yield
57	Cu	6	10.9	M10 UNC	Flange	None	85% of yield
58	Cu	6	10.9	M10 UNC	Flange	Crest cup	85% of yield
59	Cu	6	10.9	M10 UNC	Flange	None	100% of UTS
60	Cu	6	10.9	M10 UNC	Flange	Crest cup	100% of UTS
61	Cu	1	8.8	M6 UNC/ brass nut	Flange	None	50% of yield
62	Cu	1	8.8	M6 UNC/ brass nut	Flange	None	75% of yield
63	Cu	1	8.8	M6 UNC/ brass nut	Flange	Crest cup	50% of yield
64	Cu	1	8.8	M6 UNC/ brass nut	Flange	Crest cup	75% of yield

Figure 3.3 demonstrates that an hour is enough time for the temperature to begin to stabilize and reach a nearly steady-state value. It was considered to run the test for longer so that the temperature would be closer to steady-state. However, any increase in cycle time would have a large impact when considering the test would run for 100 cycles. The heating and cooling times are similar to or greater than those used in literature [2, 12, 32].

If the temperature measurement reached 170°C, then the joint was determined to reached failure criterion. This reading is similar to values used in the literature [2, 32]. Hence, when the temperature of any bolted joint reached 170°C the data acquisition software immediately turned the current off, and the test was concluded. In addition, an external ambient thermocouple with a cutoff of 90°C served as a backup in the case of main system failure.

3.2 Test Setup

The test stand was designed and run at Auburn University as seen in Figure 3.4 and Figure 3.5. The test stand consisted of a power supply that delivered DC current, busbars that delivered current to the test chamber, a test chamber (which held the busbars being tested) data acquisition equipment, and computers for data logging.

Power Supply
• Up to 860 Amps DC

Busbars and Protective Cover

Test Chamber
• 8 Pairs of busbars tested simultaneously
• Aluminum fixtures connected test pairs together in series
• Plexiglas case
• Garolite board

Fans
• High sensitivity to ambient temperature

External Thermocouple and Switch

Figure 3.4: Test setup

Thermocouple

Wiring and Mechanical Connectors
• Voltage drop

Module Carriers with Modules
• Thermocouple modules
• Voltage modules
• Relay

Two Dell computers and monitors
• Labview

Figure 3.5: Measurement equipment

The power supply delivered DC current based on the type of bars being used, as seen in Table 3.3. The values were chosen because they gave a temperature rise of approximately 100°C. Preliminary tests using various configurations were conducted to determine what current values gave the desired temperature rise.

Table 3.3: Current values

Busbar Material	Busbar Thickness (mm)	Current (A)
Copper	1	330
Copper	6	860
Aluminum	6	575

The current was cycled for 1 hour with the power on, followed by 1 hour with the power off, through the use of a relay. This process was repeated for 100 cycles, or a total of 200 hours, unless the cutoff temperature (170°C) was reached.

Copper busbars were used to connect the power supply to the test chamber, which was covered with a plastic shield for safety purposes. The test chamber was made of plexiglass, with dimensions of approximately 50"x32"x6". Inside, the chamber held eight pairs of busbars, as seen in Figure 3.5. The busbars were in a figure eight configuration, mounted on a Garolite board with dimensions of 48"x30"x0.25". Each busbar pair consisted of two bars with through holes at both ends, which were held together by a single nut and bolt as determined by the test matrix. Each pair of busbars was then connected on both ends to an aluminum fixture. All of the bars and fixtures were bolted together in series, as seen in Figure 3.6. Two of the aluminum

fixtures connected the copper busbars responsible for bringing current from the power supply and the tested busbar pairs.
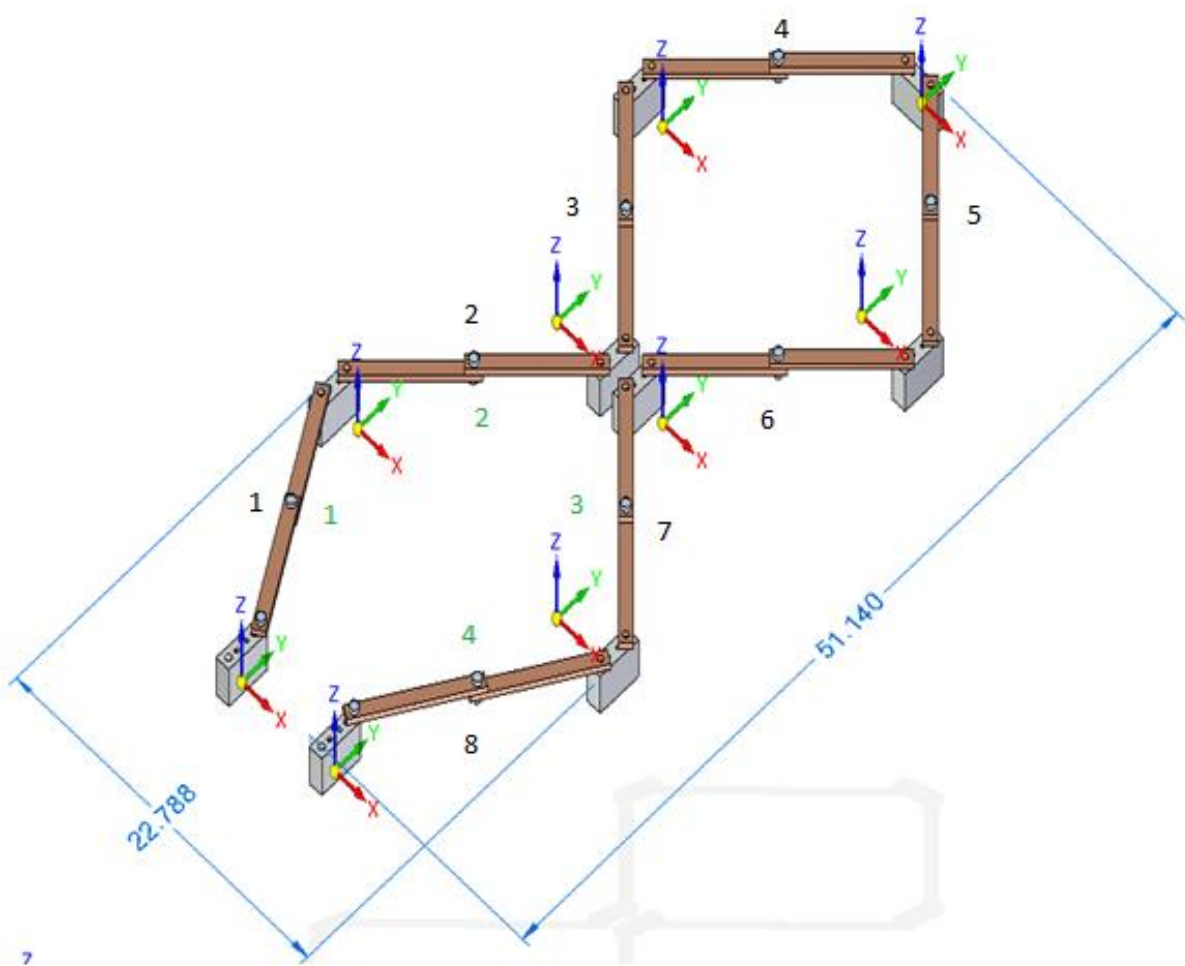

Figure 3.6: Busbar and fixture setup (all dimensions are in inches); the numbers next to the busbars are the busbar number (numbers on inside are for the smaller design)

A thermocouple was placed near the contact of each busbar pair to take temperature readings near the contact surface, thus indicating the temperature near the joint, as seen in Figures 3.7 and 3.8. The thermocouple for 6 mm thick busbars was placed in the middle of the top busbar, which gave a better contact on the flat surface, as seen in Figure 3.8. The

thermocouple for 1 mm thick busbars was placed in the middle of the two busbars, as this was the only position the thermocouple could be consistently placed. At the bar ends, voltage probes with high temperature wiring were used to measure the voltage drop across the entire bar pair, as seen in Figure 3.7. The voltage drop could then be used to calculate the busbar resistance, as in [5]. It should be noted that the resistance consists of contact resistance at the contacts and bulk resistance of the busbars. In addition, two thermocouples were used to measure the ambient temperature, one of which was independent from the rest to serve as a safety measure in the case of system failure (such as might result from the power supply being left on for an extended period of time after a contact has degraded).
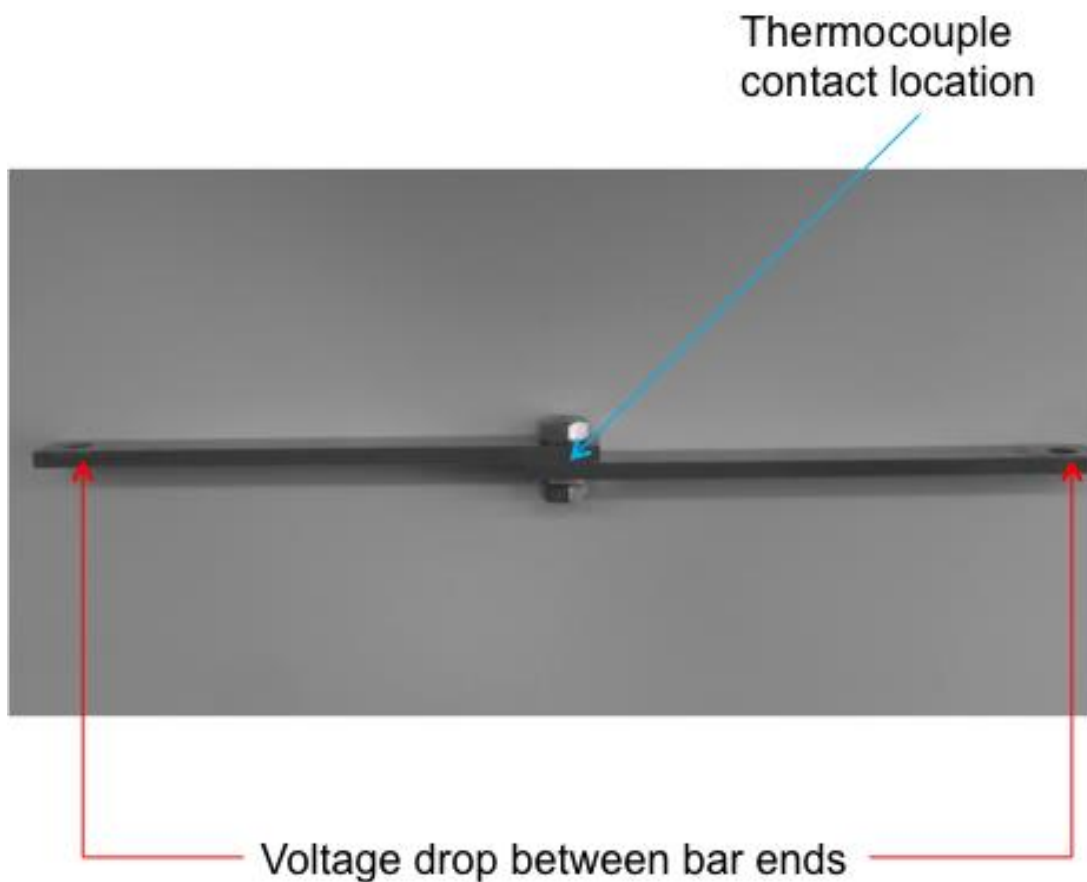

Figure 3.7: Voltage and temperature measurements on bolted joint

Figure 3.8: Thermocouple placements on 6 mm thick busbars (top) and 1 mm thick busbars

(bottom)

Six to eight small diameter fans were used to create a more uniform ambient temperature within the test chamber. Separate configurations were used for the copper busbars versus the aluminum busbars, due to their varying sensitivities to ambient temperature. Ambient temperature has a strong influence on joint resistance [10], which is also observed in the current work. There were instances where an inadequate fan configuration was used. As a result, part of the test stand would overheat and a busbar pair would exceed its temperature limitation unreasonably quickly, sometimes less than 24 hours into a test.

Six fans were placed in a random configuration, as see in Figure 3.9, for the copper busbars tests. The aluminum busbar tests had a single fan in front of the middle of each bolted joint. The copper busbar fan configuration was determined after running tests where the same case, or busbar configuration, was run at every position. The goal was for the temperature at

each busbar to be roughly the same. Different fan configurations, such as placing fans in each corner and placing fans in the same direction, were evaluated. However, a configuration where the fans are randomly displaced results in the smallest temperature difference across all locations on the test stand.

The configuration for the aluminum busbars was not the same as that of the copper busbars. A single fan was placed in front of each bolted joint as seen in Figure 3.10 for the aluminum busbar tests. A test was setup where each bolted joint was the same case again. The distance between the fans and busbars was altered to achieve the smallest temperature difference across all locations on the test stand.
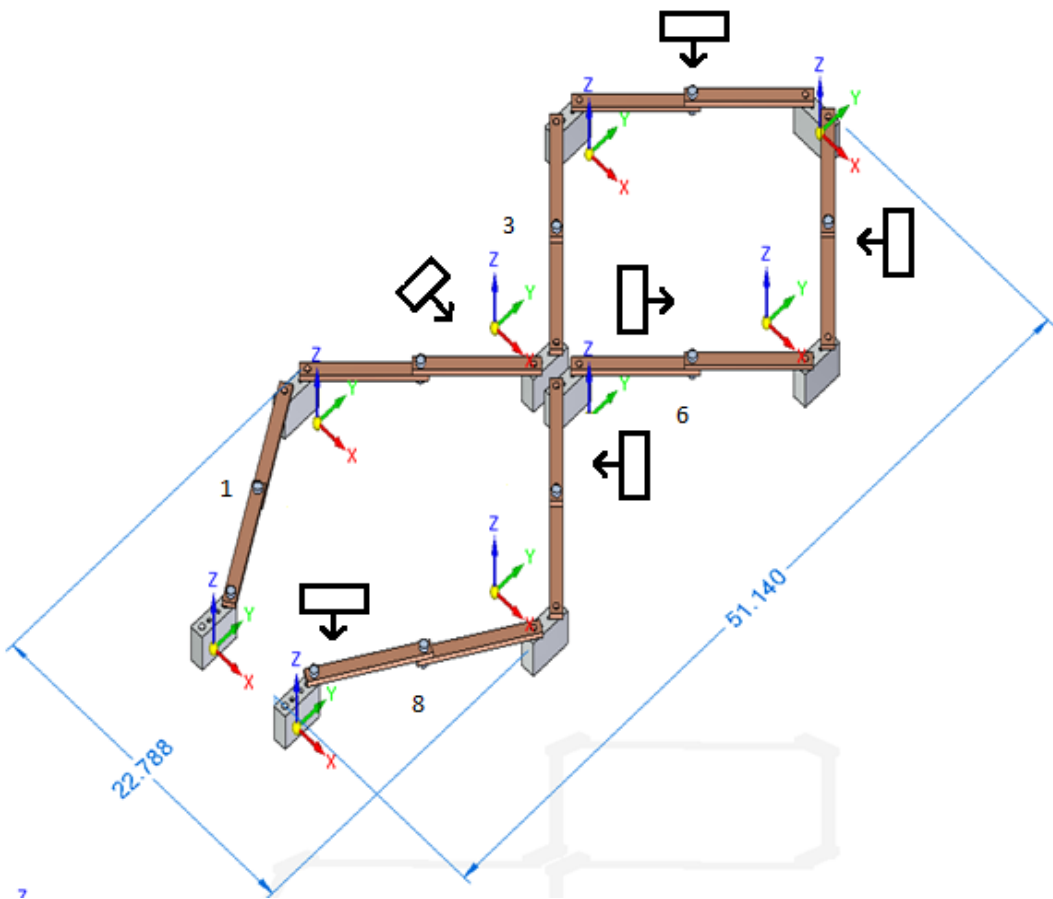

Figure 3.9: Copper busbar fan layout (all units are in inches); the numbers next to the busbars are the busbar number (numbers on inside are for the smaller design)

Fans
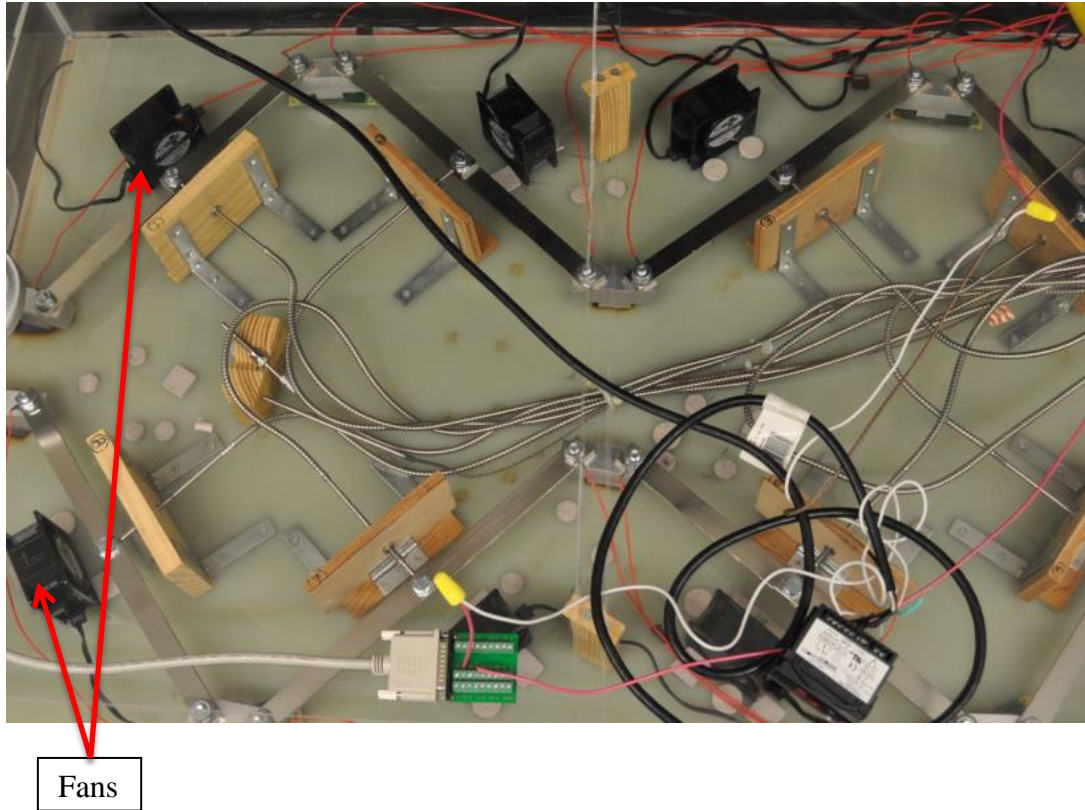
Figure 3.10: Aluminum busbar fan layout

The thermocouples, voltage leads, and relay were attached to three NI SC-2345 Module Carriers, as seen in Figure 3.11. Each module carrier could hold up to eight digital channels. One module carrier held the thermocouple modules for the busbar temperature measurements, a second held the voltage modules for the voltage drop measurements, and the third held the module for the ambient temperature thermocouple and the relay. SCC-TC02 thermocouple modules, as seen in Figure 3.10 (specifications shown in Table 3.4), SCC-AI05 voltage modules (specifications shown in Table 3.5), and relay SCC-RLY01 were used. The thermocouples for the carrier modules were K type thermocouples from Omega (BT-000-K-2 ¼-60-1 UNGROUNDED BAYONET T/C Assembly). According to ASTM E230-ANSI MC 96.1, the

error for the K type thermocouple is 2.2°C or 0.75% in the temperature range of temperatures greater than 0°C to 1250°C.
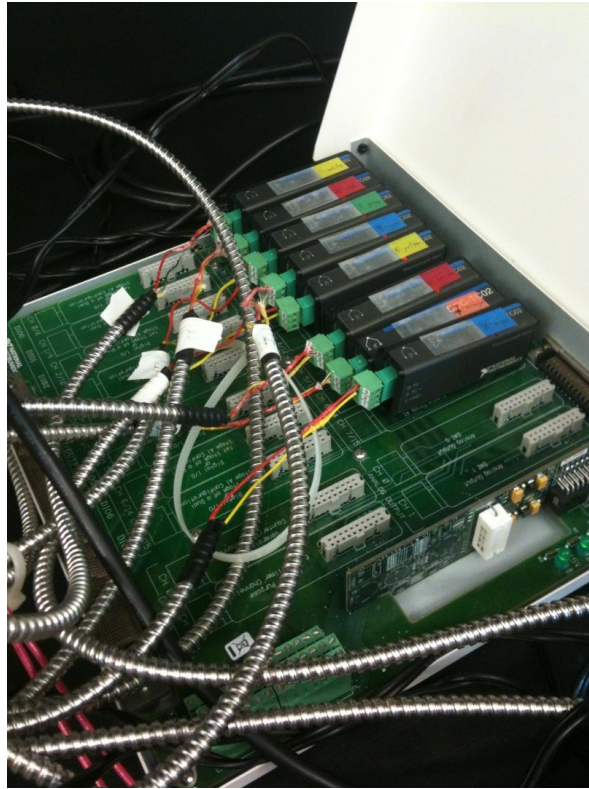

Figure 3.11: Measurement equipment

Table 3.4: SCC-TC02 specifications

Gain error	±0.08% max
Gain stability	±0.0005% °C max
Offset error	±5 µV max (post calibration)
Offset stability	±0.6 µV/°C max
Nonlinearity	±0.004% max

*For gain and offset stability the temperature range is of the module at 0 to 50°C. For gain error, offset error and nonlinearity the temperature range is 18°C to 28°C.

Table 3.5: SCC-AI05 specifications

Gain error	4.5% max
Gain stability	150 PPM/°C
Offset error	40 mV max (RTI^2)
Offset stability	225 µV/°C
Nonlinearity	0.0128% typ 0.0260% max

The temperature and voltage measurements were read with a datalogger, such as in [2, 32]. The temperature and voltage readings were recorded at 1 Hz with two Dell computers running Labview.

3.3   Profilometer

A Veeco DEKTAK 150 stylus profilometer, seen in Figure 3.12, was used to acquire roughness values on the contacting surfaces of the busbars. This is to meet the requirement specified in section 3.1, so that the effect of roughness on reliability may be correlated.

Four scans of each contact area of each test pair, as seen in Figure 3.13, were taken before each test was completed. The measurements were taken within the expected apparent contact area between the two busbars held by the bolt head and nut, where the pressure is the highest and can generate a-spots [8].
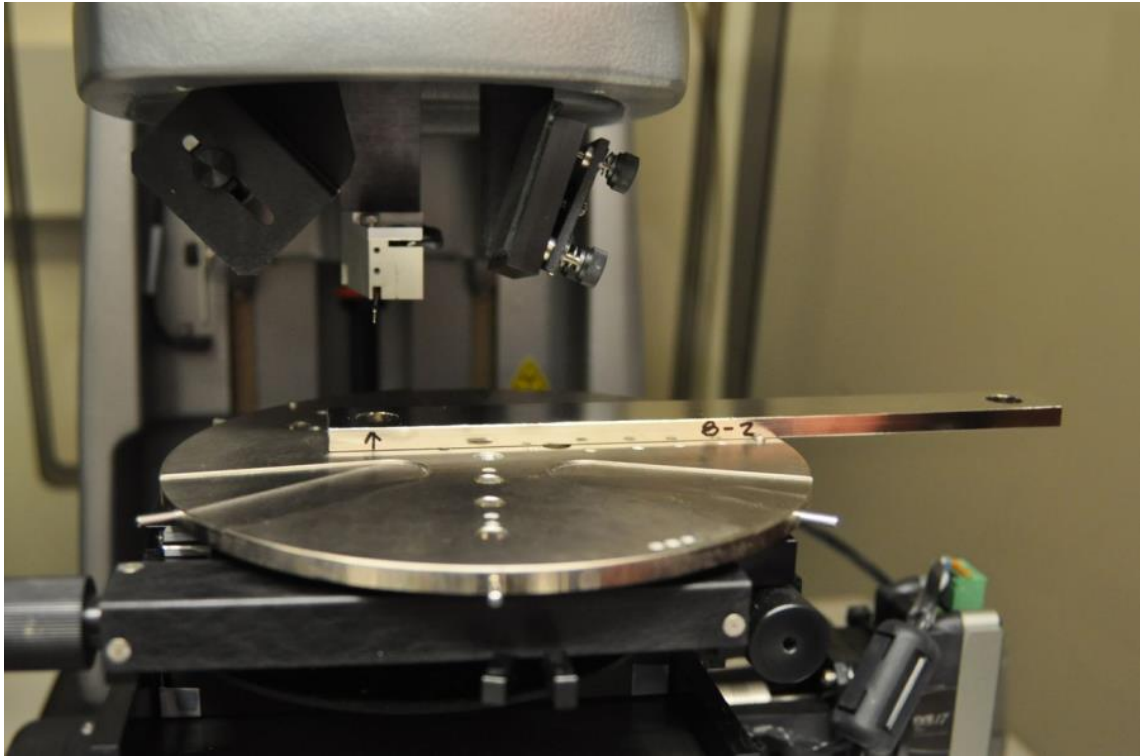
Figure 3.12: Profilometer
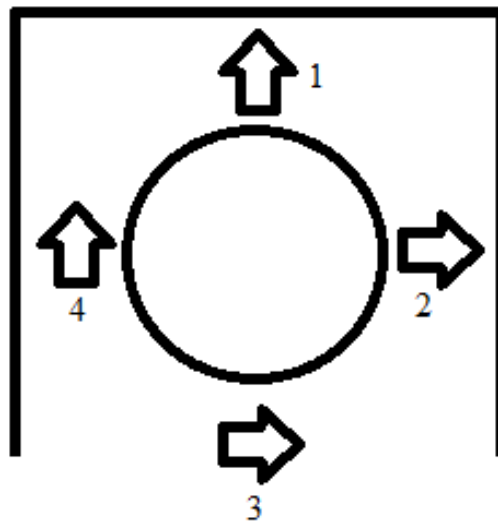
Figure 3.13: Profilometer scanning paths

These profilometer scans were used to calculate the root mean square roughness, R_q, Matlab™ using the scan characteristics as seen in Table 3.6. In the equations below L is the sample length and z is the vertical position as read by the profilometer.

The root mean square figure is given by

$$R_q = \sqrt{\frac{1}{L} \int_0^L z^2 dz} \tag{15}$$

The four roughness values, from the four profilometer scans, were then averaged together to approximate the effective roughness value of each contacting surface. After this the magnitude of the values was calculated to get the equivalent roughness. The equivalent roughness values were what were used in the data analysis.

$$R_{q,eq} = \sqrt{R_{q,1}^2 + R_{q,2}^2} \tag{16}$$

Last, measurements were taken after each test was completed so that the change in roughness could be studied.

Table 3.6: Profilometer specifications

Scan length	3800μm
Sample length	0.5μm
Tip radius	2.5 μm
Measurement Range	524 μm
Lateral gridsize	0.500 μm/sample
Vertical resolution	80 Å
Force	10.00 mg

3.4   Test Results

A sample of a single test is shown in Figure 3.15. The top graph is the maximum temperature value of each cycle for each thermocouple reading. T1 through T8 represent the temperatures of the different bar pairs within the test chamber (in a clockwise order beginning with where the power supply connects with the test chamber). The graph in the middle is the minimum temperature value of each cycle for each thermocouple reading (T1-T8). The bottom graph displays the voltage drop readings of each busbar pair (V1-V8). V1 through V8 were the voltage drops across each busbar pair during a test in the same order as the temperature measurements.

This graph shows that pair 6 (the magenta line) underwent a rapid increase in voltage drop and maximum temperature approximately two-thirds of the way through the test (at 53 cycles) until it reaches the cutoff temperature of 170°C. It can be concluded that the joint exceeded its limitations due to the rapid increase of both temperature and resistance.

The effects of joint degradation are not only seen in changes in temperature and resistance. In addition, there are visual signs, such as in Figure 3.14, where the bolt has discolored due to current cycling.

Figure 3.14: Discolored bolt (right) versus new bolt (left)
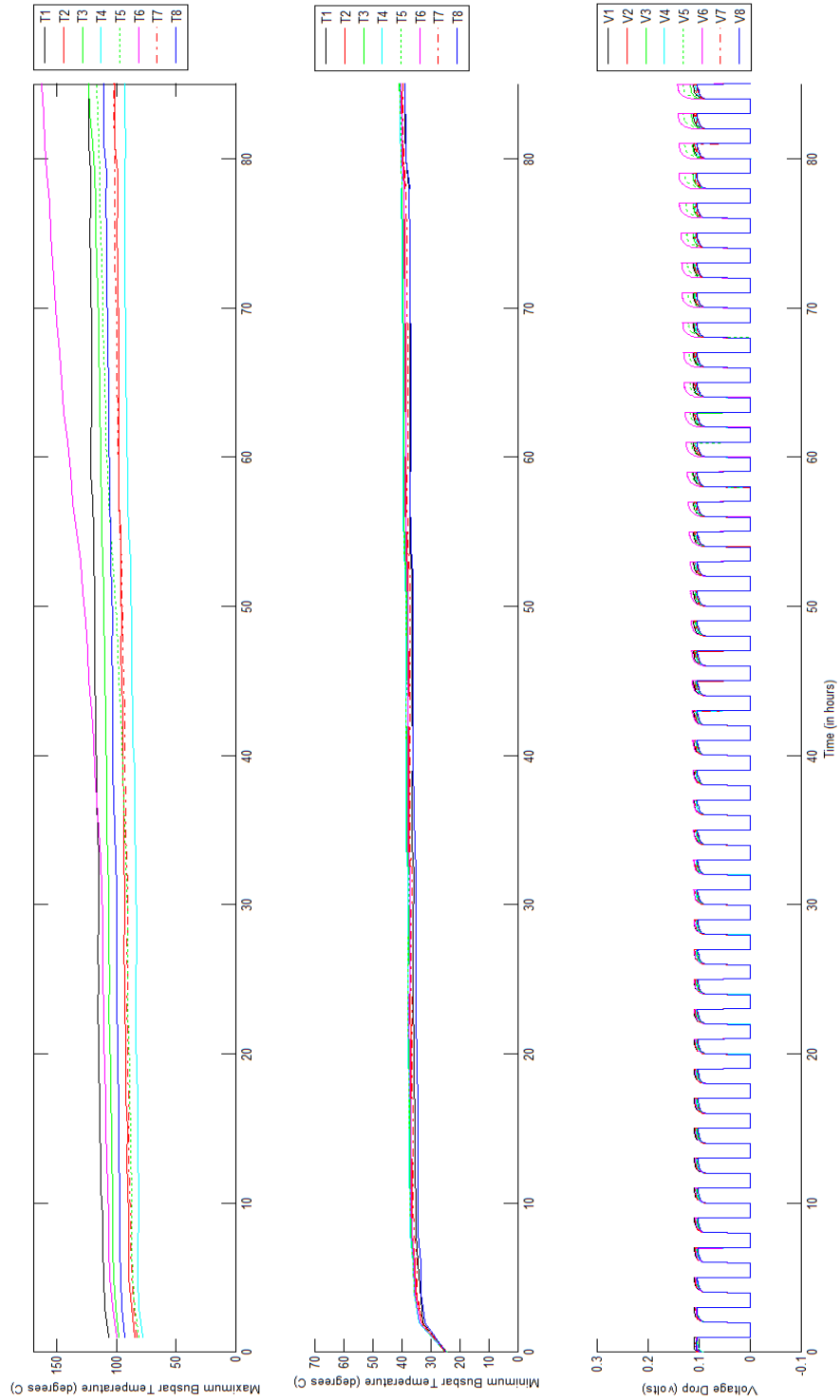
Figure 3.15: Measurements from eight busbar pairs during a test; readings from top to bottom 1) maximum thermocouple reading from each cycle, 2) minimum thermocouple reading from each cycle, 3) voltage drop

38

A sample of one cycle of one test is shown Figure 3.16. The top graph shows the temperature of a thermocouple in contact with a busbar (red dot-dash line) and a thermocouple that measures ambient temperature (green dash line). Below that is the voltage drop, followed by the current, which is represented as a step function. Last, the resistance across the joint is displayed. It should be noted that the resistance increases as the temperature increases.   This is due to the temperature and resistivity being linked to each other. As current flows through a joint, the temperature increases.   However, as the temperature increases the heat causes an increase in resistivity. This could be due to both an increase in resistivity and thermal expansion. Thus, both the temperature and resistance graphs have a positive slope in each cycle and the two are related to each other.   Accordingly, the type of joint that has a greater slope will be less reliable due to its inclination to heat up and for the contact resistance to increase.
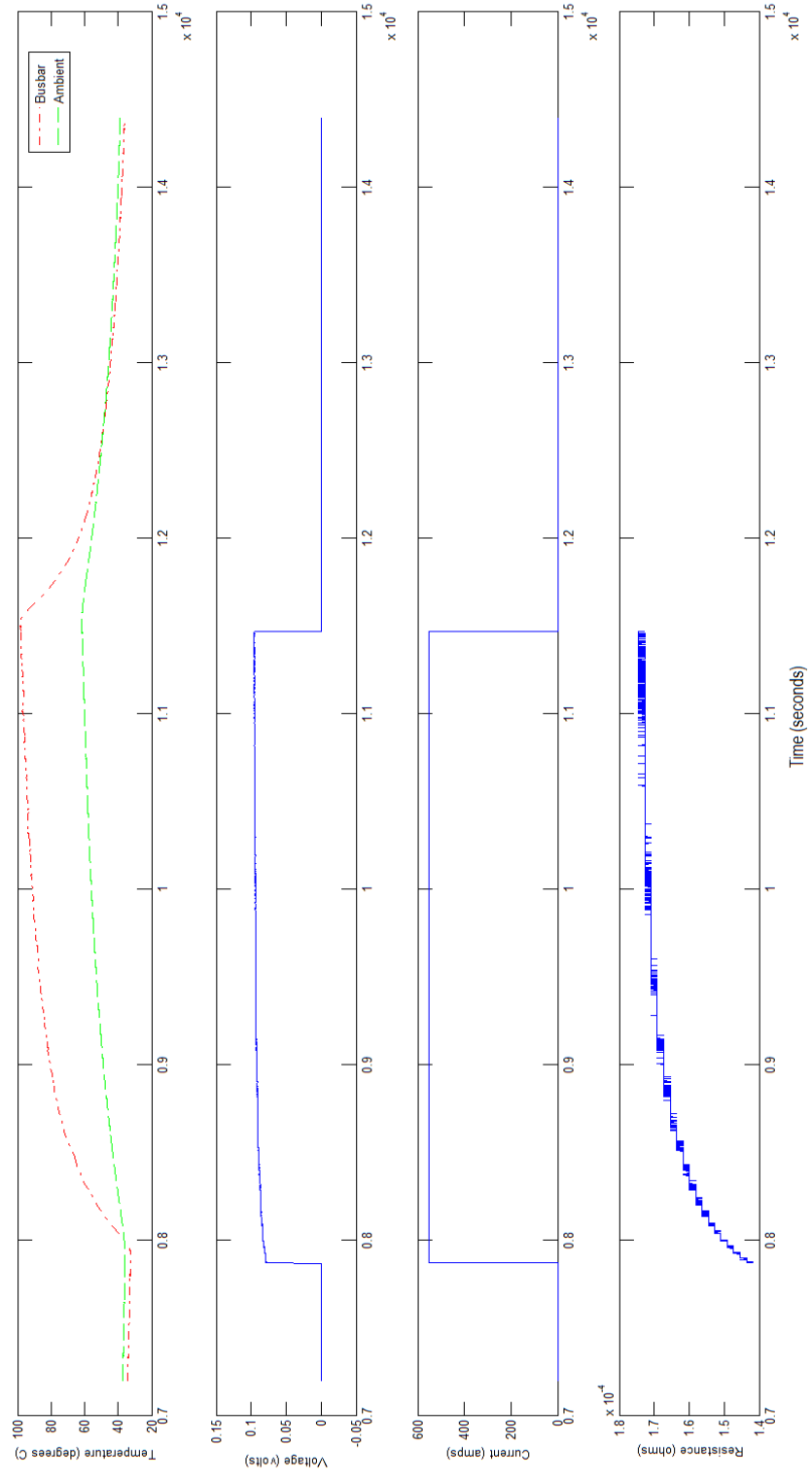
Figure 3.16: Measurements of one busbar pair from a single cycle of one test; readings from top to bottom 1) temperature, 2) voltage drop, 3) current flow, 4) resistance

Chapter 4

Statistical Analysis

The purpose of this research was to determine the most advantageous material combinations for improving reliability by reducing the resistance rise and temperature rise in high-power bolted joints. In order to examine the relationship between material combinations and reliability, a multiple linear regression method was used to conduct the data analyses using SAS™ software. This method identified which of the material properties, or combinations of variable properties, were significant in increasing or reducing temperature rise and resistance rise. In addition it expressed these significant relationships as a linear relationship. Furthermore, the multiple linear regression method allowed for the prediction of temperature and resistance rise based upon known material combinations and the applied torque on the busbar joints. The regression model explained throughout this study could enable engineers and researchers to develop connections able to withstand the generated heat and thermal expansion over many cycles through time.

A statistical analysis was performed on the bolted joints test data from Chapter 3. However, prior to analysis the voltage drop data was converted to resistance. In addition, MATLAB™ was used to calculate the change in resistance (resistance rise) and change in temperature (temperature rise) for analysis. Due to the large number of tests that ended early for 6 mm copper busbars, some results were predicted based on test data. Temperature rise is defined as the difference between the maximum temperature values recorded from the second half of each test and the maximum temperature value recorded from the first half of each test. Resistance rise is defined as the difference between the mean of resistance from the second half of each test and the mean of resistance from the first half of the test. The one exception to this

was maximum resistance rise was for 6 mm copper busbars due to a better correlation with the results. In this case the difference in the maximum resistance value recorded from the second half of each test and the maximum temperature value recorded from the first half of each test was used. The final designations were used because they gave the best results through trial and error.

Additionally, for all cases, there were some variations in temperature and resistance rise based on the location of the bolted joint in the test chamber. Hence, the average temperature rise and resistance rise were calculated for each position of each bar type. Next, the temperature rise and resistance rise of each tested joint was subtracted from the average temperature. This resulted in a relative temperature rise and relative resistance rise, and served to compensate for parts being tested at different locations within the test chamber.

Due to the different applied currents, fan configurations, and geometries for each busbar type, separate analysis was performed on the three different types of busbars which were tested: 1 mm thick copper busbars, 6 mm thick copper busbars, and 6 mm thick aluminum busbars. This is also how this chapter will be organized after further discussion of multiple linear regression analysis and an explanation of how the analysis will be performed.

4.1 Multiple Linear Regression Analysis

The *regression* of Y (response variable) on X_1, X_2, X_3 etc. (predictor variables) is a rule that explains the distribution mean of a response variable (Y) for predictor variables ($X_1,X_2,\ldots$). A linear regression model is one whereby the relationship between the response and predictor variables is expressed linearly [33]. A linear regression statistical model [34]could be expressed as

$$y = \beta_0 + \beta_1 x + \varepsilon \qquad\qquad (17)$$

where y is the response variable, x_i is a *regressor* or *predictor* variable, β_0 and β_1 are *regression coefficients* (β_1 is the change in mean of the distribution of the response, or the slope, and β_0 is the mean of the distribution of the response when all predictor variables are zero, or the y-intercept) and ε_i is a component of random errors [34].

Multiple linear regression is linear regression for two or more predictor variables and one response variable [33]. For the purpose of this work six predictor variables are used. The six predictor variables are class of steel, head type, presence of a Belleville washer, applied torque, roughness, and nut material. Therefore

$$y = \beta_0 + \beta_1 x_1 + \beta_2 x_2 + \beta_3 x_3 + \beta_4 x_4 + \beta_5 x_5 + \beta_6 x_6 + \varepsilon \qquad (18)$$

where y is temperature rise or resistance rise, x_1 is the class of steel, x_2 is the head type, x_3 is the presence of a Belleville washer, x_4 is the applied torque, x_5 is the roughness, and x_6 is the nut material.

In addition, interaction terms are added to create a full model. An interaction term takes into account whether the response changes when one predictor variable depends on the other [33]. The interaction term consists of a β variable and some combination of predictor variables multiplied together. For example, if x_5 and x_6 were combined then the model would appear as

$$y = \beta_0 + \beta_1 x_1 + \beta_2 x_2 + \beta_3 x_3 + \beta_4 x_4 + \beta_5 x_5 + \beta_6 x_6 + \beta_7 x_5 x_6 + \varepsilon \qquad (19)$$

4.2 Analyzing Results

While performing statistical analysis the data can be studied multiple ways. First, the raw data can be observed. This is done using methods such as scatterplots, boxplots and torque graphs. After the raw data is studied, multiple linear regression analysis is performed. Multiple linear regression analysis encompasses proving assumptions necessary to perform multiple linear

regression analysis, possible transformations that might be required to perform multiple linear

regression analysis, followed by the analysis itself.

4.2.1   Scatterplots

A scatter diagram is a plot of two variables. It encompasses all observations, such as in

Figure 4.1, and can indicate a relationship between two variables [34]. In the example in Figure

4.1, the roughness and temperature rise appear to be positively correlated. This is also known as

a scatterplot.
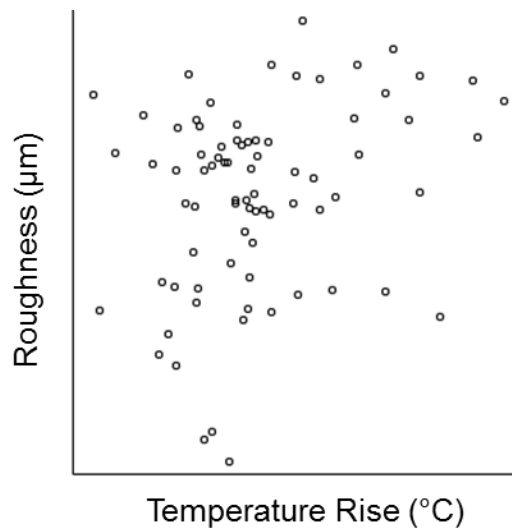
Figure 4.1: Scatterplot example

A scatterplot is a major tool for assessing a model. It is used to demonstrate problems of

the linearity assumptions and constant variance assumption, which will be discussed later in the

chapter. A scatterplot is helpful in observing the relationship between two variables and can

bring attention to noteworthy points and signify the necessity of a transformation [33].

A scatterplot is also helpful in determining patterns, as seen in Figure 4.2 below. The scatterplot shows that there is a relation between roughness and temperature rise: as the roughness increases, the temperature rise increases.

4.2.2   Boxplots

Another way to present numbers is a *box plot*, as see in Figure 4.2. A box plot graphically shows the middle 50% of data using a box. The lower and upper 25% are displayed using other symbols. The graph shows the skewness, spread and center of the data, in addition to outliers [33].

The middle 50% of the data, or difference in upper and lower quartiles, is known as the *interquartile range* (IRQ), and is shown by a box. The lie across the middle of the box is the media. The line on the lower part of the graph is the minimum value if it is no more than 1.5 box-lengths from the bottom of the box. The top line is the maximum value if no more than 1.5 box-lengths from the top of the box. The values that are represented by dots are those outside 1.5 box-lengths from the box. Box plots displaying differences in distributions may be placed next to each other, and are known as side-by-side box plots [33].

4.2.1   Assumptions

The accurate explanation of statistical statements depends on four regression model qualities (assumptions): normality, linearity, constant variance, and independence [33].

The linear assumption is violated when a straight line is insufficient to describe the regression, or there are one or more outliers, which stem from different populations that make it unsuitable to use the complete data set. A scatterplot may be used to show difficulties in nonlinearity [33].
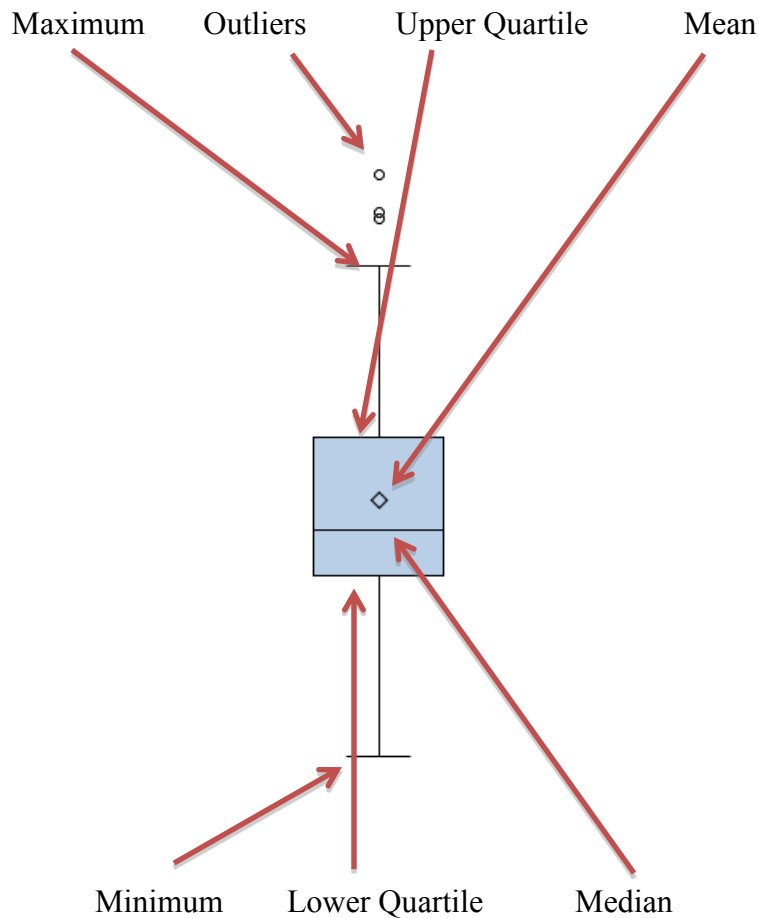
Figure 4.2: Boxplot example

Second, the constant variance assumption assumes the spread of response points about the straight line is identical at all explanatory variable values. If this assumption is violated then confidence intervals and tests could be deceptive. A scatterplot of residuals versus fitted values can warn whether there is nonconstant variance [33].

Third, the normality assumption assumes the responses of subpopulations at various explanatory variable values have normal distributions. The estimates of coefficients, along with their standard errors, are robust to distributions that are no normal, unless there are outliers. However, nonnormal distributions are critical if prediction intervals are used [33]. The Kolmogorov-Smirnov test is a normality test used by SAS™. If the P-value is greater than the

critical value (assumed in this thesis to equal 0.05), then the data can assume to have come from an indicated distribution (website)

Last, the independence assumption assumes the position of the response relative to its mean cannot be projected through knowing the position of other responses relative to their means. Standard errors are affected if this assumption is not met [33].

4.2.3 Box-Cox Transformation

It is possible to transform y if there is a problem with nonconstant variance or nonnormality. One transformation is the power transformation method, y^λ, where λ is a determined value. Box and Cox showed how the value λ and the regression model parameters could be estimated simultaneously. The method of using the transformation [34] is

$$y^{(\lambda)} = \begin{cases} \frac{y^\lambda - 1}{\lambda \dot{y}^{\lambda-1}}, \lambda \neq 0 \\ \dot{y} ln y, \lambda = 0 \end{cases} \qquad (20)$$

and

$$\dot{y} = ln^{-1}[\frac{1}{n \sum_{i=1}^{n} ln y_i}] \qquad (21)$$

4.2.4 Variable Selection

There are many tools accessible for reducing large series of explanatory variables. The first step in a sequential procedure begins with a current model. Next, a similar model (one with one greater or one fewer variable) is tested to determine which is better. The best model is picked and the process repeats, with the selected model becoming the new current model. Three

sequential variable selection techniques are: forward selection, backward elimination, and stepwise regression [33].

The forward selection method begins with a constant mean for its current model. It then adds an explanatory variable one at a time until no addition of variables (significantly) improves the fit [33]. The backward elimination method starts with every possible explanatory variable. The significance for each variable is calculated. The variable that is the least significant is eliminated and the process is repeated until only significant variables remain [33]. The stepwise regression model consists of performing one step of forward selection followed by one of backward elimination. This is repeated until explanatory variables cannot be removed or added [33]. The results from the different methods are compared to determine the final results.

The final statistical model is simplified into a reduced model using the statistical program, SAS™. This is done using forward, backwards and stepwise elimination. The reduced model is used to determine the parameter estimate, **β,** of each significant variable, along with the standard error. Thus, at the end of multiple regression analysis the following information is known: the significant variables (or combination of variables), the parameter estimate of all significant variables, and the standard error of all significant variables.

4.3 Explanation of Variables

This thesis deals with the six predictor variables: steel class, surface roughness, initial applied torque, washer presence, bolt head type and nut material. The steel class is used to describe the strength of steel used in the nut and bolt. The material and size of the clamping bolts is important because the maximum compressive force the bolt and nut exert depends mainly on the bolt's tensile strength, degree of tightening, and pitch of threads [7]. There are

three types of steel used in the experiments; therefore a categorical variable will be used. In the example of 1 mm copper busbars, class 4.8 bolts will be represented with a 0, class 8.8 bolts will be represented with a 1, and class 10.9 bolts will be represented with a 2.

Roughness is another variable used in the analysis. It is known that real surfaces are not perfectly smooth but possess many asperities. Therefore, when there is contact between metals, these asperities will form local metallic contacts. These are the paths electricity flow through [4]. A rougher surface that contains more severe asperities will have a greater probability of having metallic contacts and the ability to have more contacts at subsequently lower loads compared to a smooth, machined surface with a greater current-carrying area. Therefore, surface roughness is important [9, 11]. For this project a Dektak 150 Stylus Profilometer in the Multiscale Tribology Laboratory was used to take measurements of the busbar's surface profile. These readings were used to create a roughness value.

The initial applied torque was applied on the nut and bolt using a digital torque wrench. The torque readings were done as a function to the bolt's yield strength. The torque is important because it affects the force holding the joint together. When the force is increased, the area and number of metallic contact spots increases. The spots are the only paths the electrical current flow through [4].

A washer is added to give an even pressure distribution [7]. The only options tested are whether a washer is present or not; therefore, this is a categorical variable in the test. A picture of a Belleville washer is shown in Figure 4.3. As Figure 4.3 shows, the washer is curved. When a load is applied the washer deforms, acting similar to a spring. The amount of deflection is dependent on the applied load.

49

Figure 4.3: Washers [35]

The bolt head type refers to the shape of the bolt head. There are two or three types of heads used depending on busbar material, shown in Figure 4.4. Once again, because there are only two or three types, a categorical variable is used. The 6 mm aluminum and 6 mm copper busbars test hex and flange head type, as seen in Figure 4 below, while 1 mm copper additionally tests pan head machine screws.
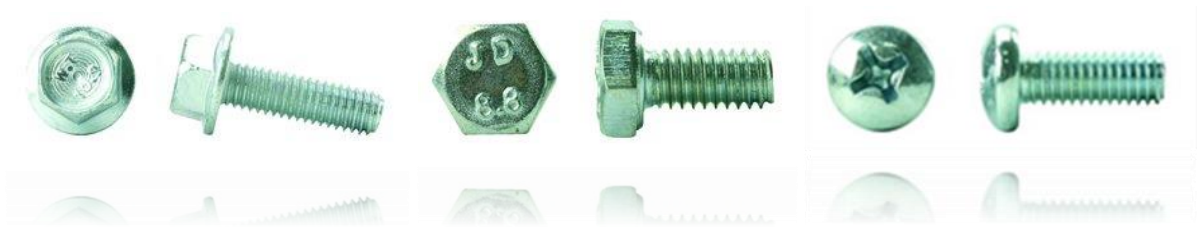
Figure 4.4: Flange head (left) versus hex head (middle) versus pan head (right) types [35]

The head type is important because it affects the surface area the load is distributed across, much like a washer would.

The nut material refers to 1 mm copper busbars with a class 8.8 hex head bolt only. The use of a brass nut, rather than the usual steel nut, was tested. Brass is a better thermal conductor, therefore it is able to dissipate heat easier. In addition, it has lower friction which could allow for a great normal force (and lower torque). However, the threads of the brass could exceed their

limitations prematurely, which would decrease reliability. A dummy variable is used to represent whether the nut material is steel or brass.

4.4 Analysis of 6 mm Copper Busbars

All of the assumptions were satisfied for the 6 mm copper busbars. However both the temperature rise and resistance rise underwent a Box-cox transformation so the normality assumption would be satisfied. In addition, many of the tests ended early. As a result, the temperature rise and resistance rise readings were analyzed for 75 cycles only. As a result, only parts of some tests (those that last longer than 75 cycles) were analyzed. In addition, the tests that lasted for less than 75 cycles had a line fit to the data to predict what the temperature and resistance values would have been at the 75th cycle. The line was fit to the maximum temperature and resistance value of each cycle. Therefore, the temperature rise was defined as difference in averages of the maximum temperature values from the first 50 cycles and the last 50 cycles. The resistance rise was defined as the difference in the average resistance of the first 50 cycles and the last 50 cycles.

4.4.1 Temperature Rise Analysis

First, the raw data was analyzed which could show possible relationships. Figure 4.5 shows the average relative temperature rise by case, which shows correlations that might take place. It is apparent that the higher torque values could result in a lower temperature rise (see red circle). The nomenclature is shown in Table 4.1

Table 4.1: Torque graph nomenclature

| Y/N	Y = A washer is present
	N = A washer is not present
S/B (1 mm copper only)	S = Nut is made of steel
	B = Nut is made of brass
4.8/8.8/10.9	Class 4.8, 8.8, 10.9
Hex/Pan/Flange	Hex, Pan, or Flange Head Types
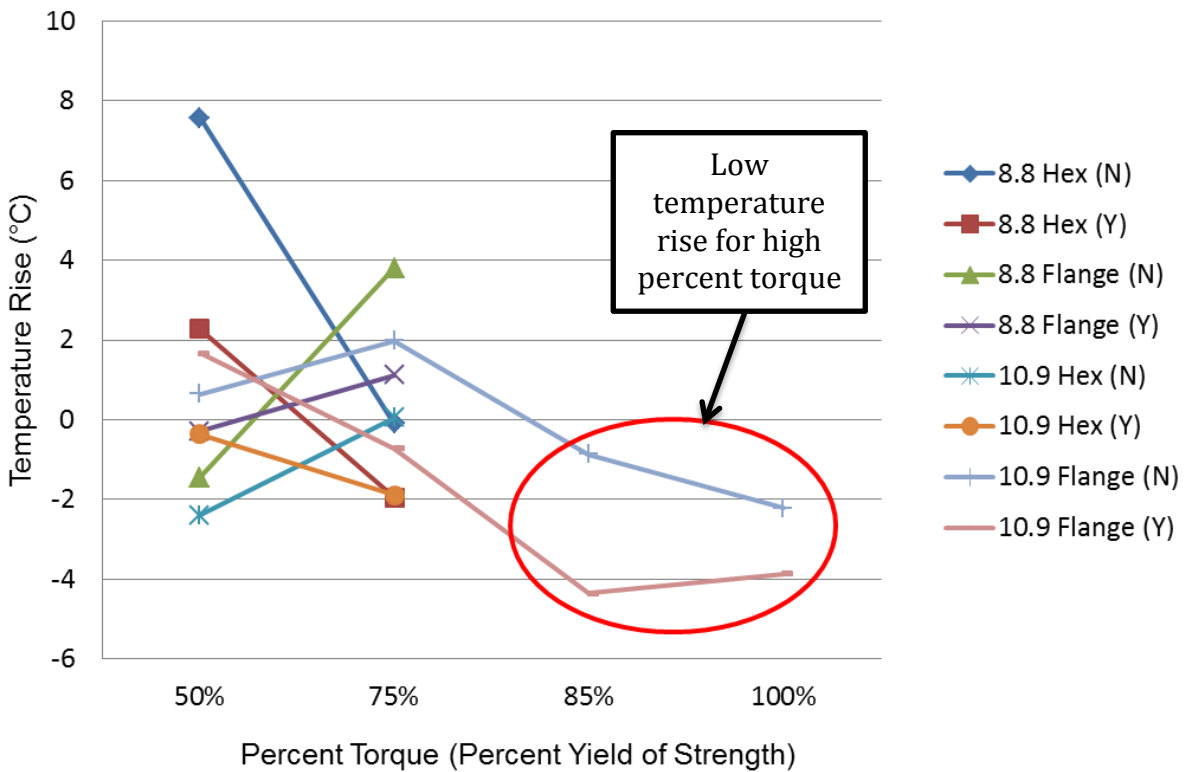
Figure 4.5: Torque graph of all 6 mm copper busbars

In addition, when the data is split up by head type for simplicity in Figure 4.6 and Figure 4.7; the effect of torque is still apparent.
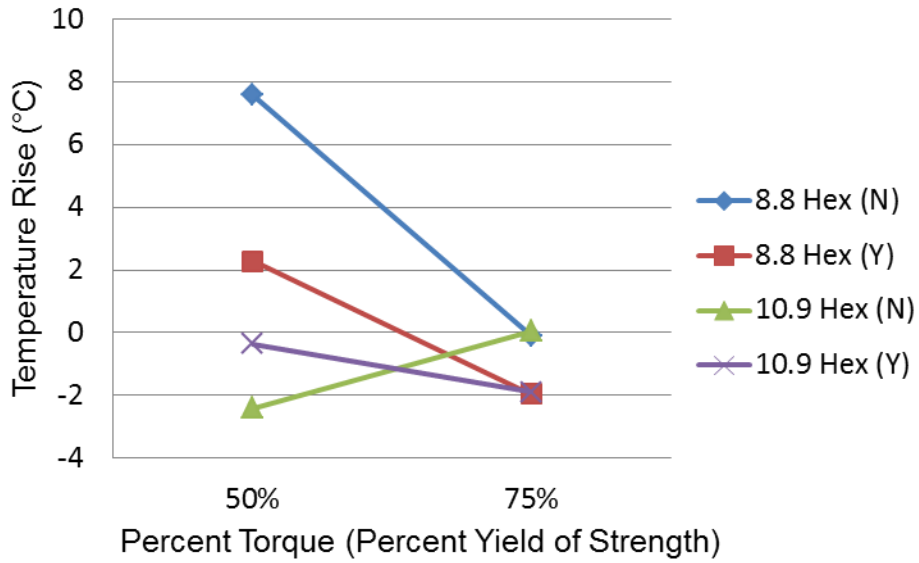
Figure 4.6: Torque graph of hex head 6 mm copper busbars
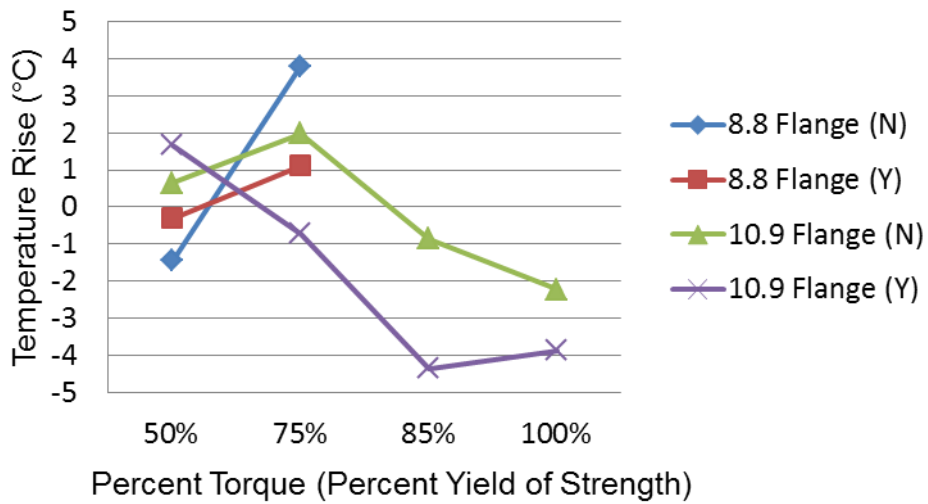
Figure 4.7: Torque graph of flange head 6 mm copper busbars

The relationship between roughness and temperature has a small relation, as seen using a scatterplot, seen in Figure 4.8
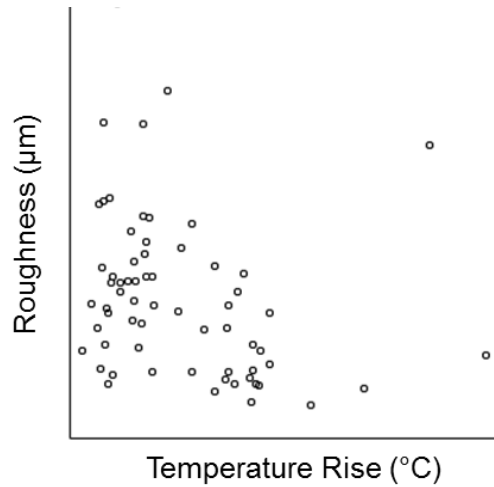
Figure 4.8: Scatterplot of 6 mm copper busbars, temperature rise

Next, forward selection, backward elimination, and stepwise regression were performed. The results are shown in Table 4.2. It is concluded that the variables head type and roughness are significant.

Table 4.2: Temperature rise, 6 mm copper busbars

Variable	Full (°C/variable unit)	Forward /Stepwise (°C/variable unit)	Backward (°C/variable unit)
Intercept	3.87 (0.79) *	3.57 (0.34)	3.06 (0.42)
Class	0.19 (0.40)	-	-
Head	-1.74 (0.70) *	-	-1.68 (0.69)
Washer	-0.25 (0.28)	-	-
Torque	-0.01 (0.01)	-	-
Roughness	-0.08 (0.15)	-0.36 (0.11)	-0.17 (0.13)
Roughness*Head	0.76 (0.25) *	-	0.69 (0.24)

* - data was significant in full model; values are parameter estimate (standard error); the standard error is the projected standard deviation of the sampling distribution of the least squares estimates [33]

4.4.2 Resistance Rise Analysis

The process for resistance rise analysis was repeated from the temperature rise analysis. Once again the raw data is analyzed in Figures 4.9, 4.10 and 4.11. Analyzing the raw data, the high torque values appear to decrease the response.
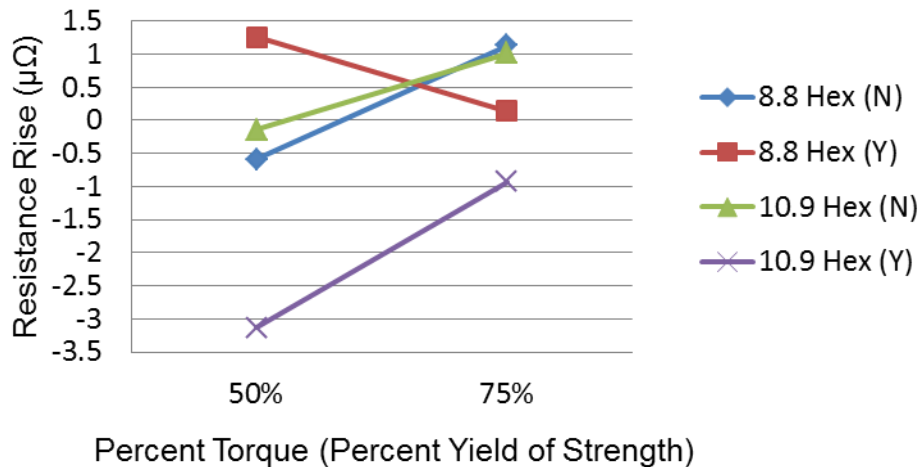

Figure 4.9: Torque graph of hex head 6 mm copper busbars
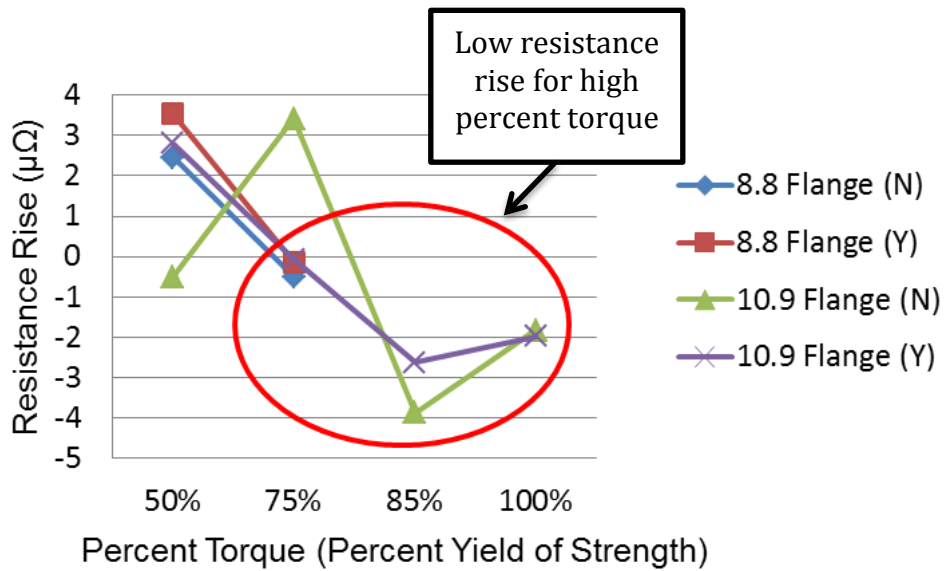
Figure 4.10: Torque graph of flange head 6 mm copper busbars
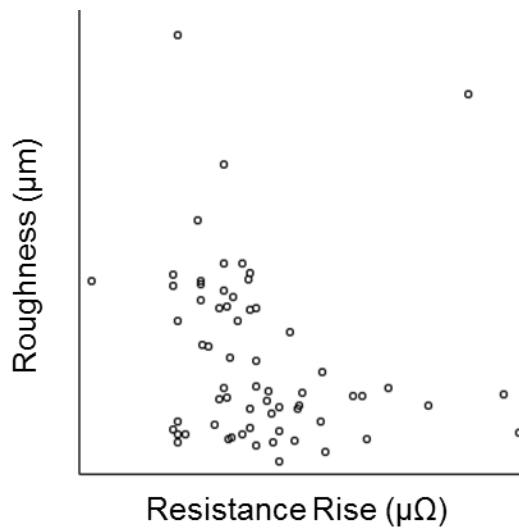
Figure 4.11: Scatterplot of 6 mm copper busbars, resistance rise

Next, forward selection, backward elimination, and stepwise regression were performed. The results are shown in Table 4.3. It is concluded that the torque variable is significant. In

addition the value is negative, hence an increase in torque will result in a decrease in resistance rise.

Table 4.3: Resistance rise, 6 mm copper busbars

Variable	Full (μΩ/variable unit)	Forward /Backward/Stepwise (μΩ/variable unit)
Intercept	4.96 (0.87) *	4.90 (0.48)
Class	-0.07 (0.43)	-
Head	-0.64 (0.77)	-
Washer	0.02 (0.31)	-
Torque	-0.02 (0.01)	-0.016 (0.007)
Roughness	-0.01 (0.16)	-
Roughness*Head	0.36 (0.28)	-

* - data was significant in full model; values are parameter estimate (standard error)

4.5 Analysis of 1 mm Copper Busbars

All of the assumptions were satisfied for the 1 mm Copper busbars. However the resistance rise underwent a Box-cox transformation so it would satisfy the normality assumption. The temperature rise was for the test was defined as the difference in the average of the last 50 maximum values and the average of the first 50 maximum values.

$$Temperature\ Rise = \ Average\ T_{max,\ 2nd\ half} - Average\ T_{max,\ 1st\ half}$$

The resistance rise was defined as the difference in the average electrical resistance of the second half of the test and the average electrical resistance of the first half of the test.

$$Resistance\ Rise = \ R_{mean,\ 2nd\ half} - R_{mean,\ 1st\ half}$$

4.5.1 Temperature Rise Analysis

First, the raw data was analyzed which could show possible relationships. Figure 4.12 shows the average relative temperature rise by case. It is apparent that the addition of a brass nut lowers the response (red circle). In addition, the flange and pan head types appear to lower the response relative to the hex head cases (black circles).
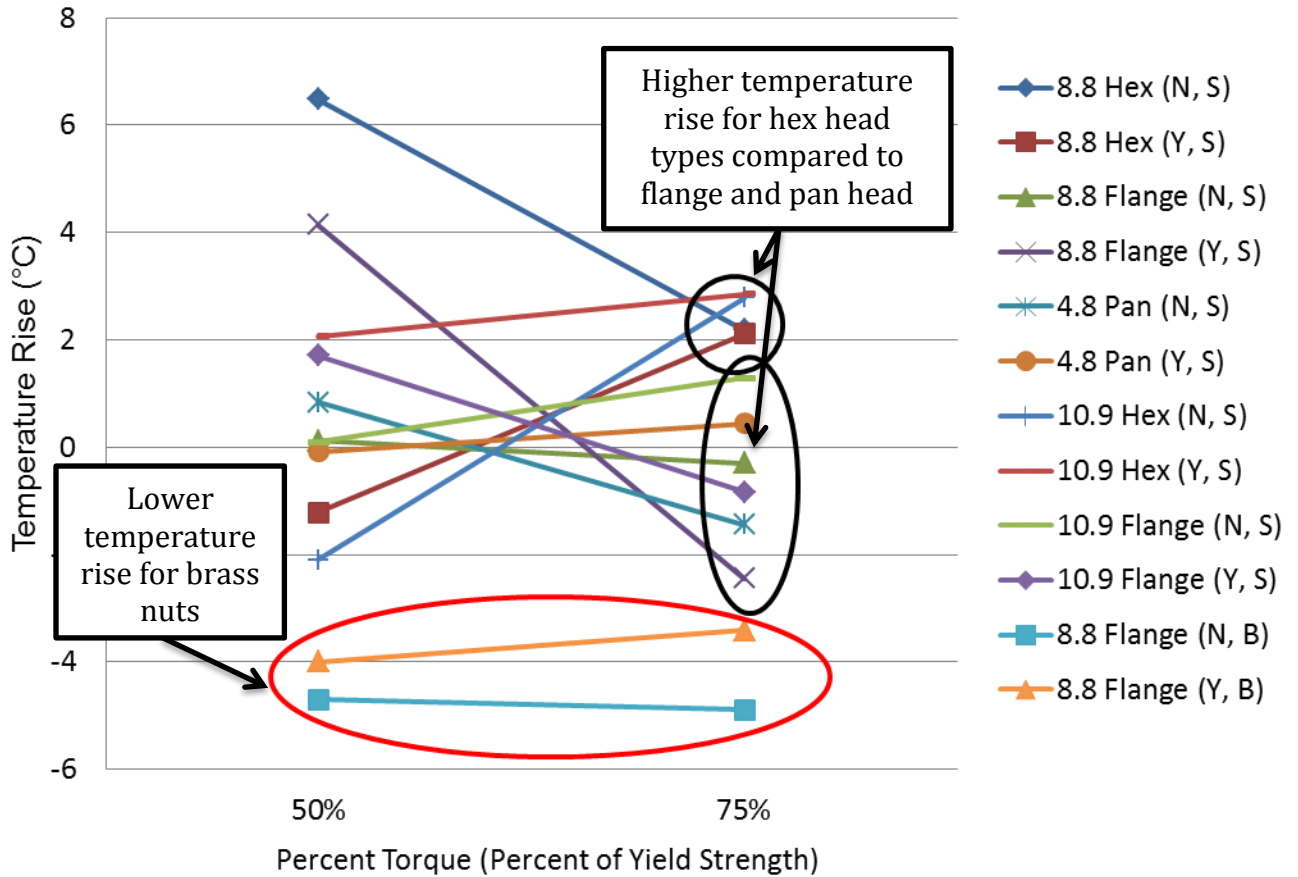

Figure 4.12: Torque graph of all 1 mm copper busbars

In addition, when the data is split up by head type for simplicity in Figure 4.13 and Figure 4.14; the effect of nut material and head type are still apparent.

58
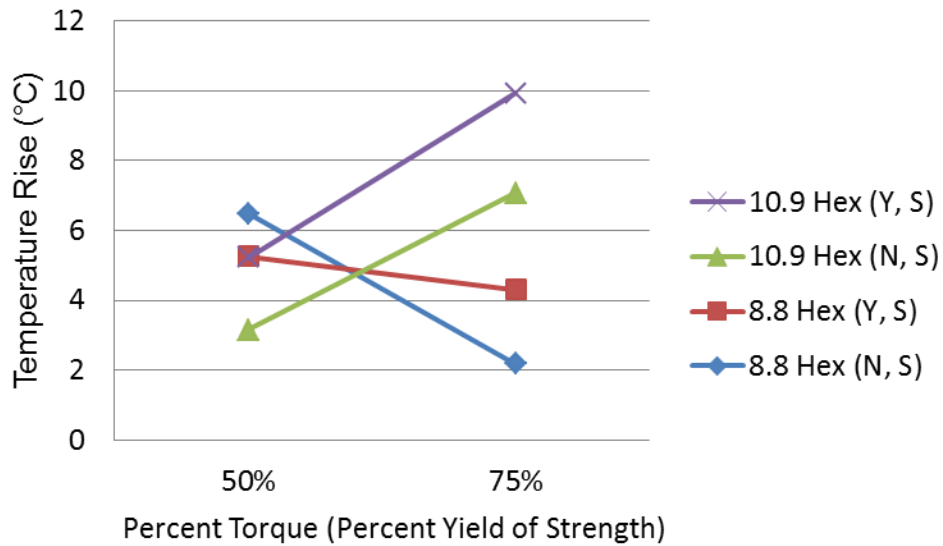
Figure 4.13: Torque graph of hex head 1 mm copper busbars
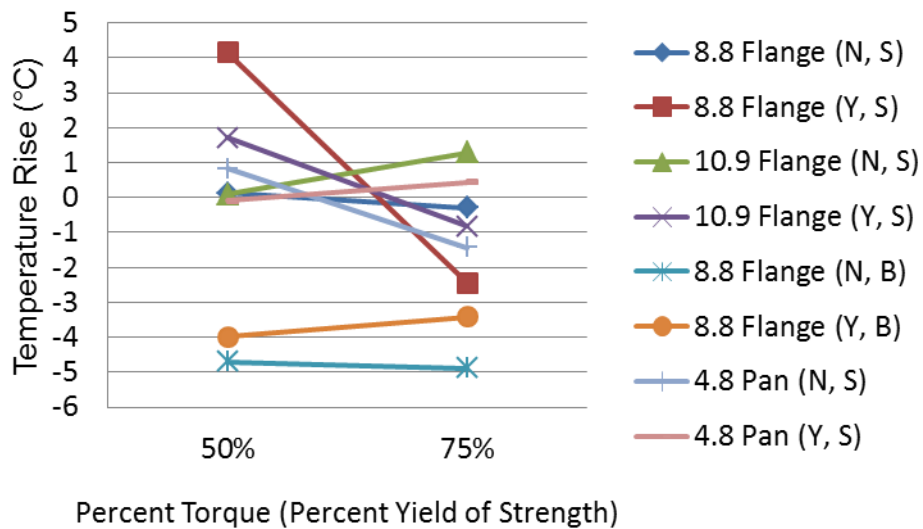
Figure 4.14: Torque graph of flange and pan head 1 mm copper busbars

A separate graph was made that only contains the cases with the brass nut option (class 8.8, flange head type cases). This graph, Figure 4.15, compared the use of a steel nut and that of

a brass nut. It is very apparent that the use of a brass nut will results in a lower temperature rise compared with the steel nut.
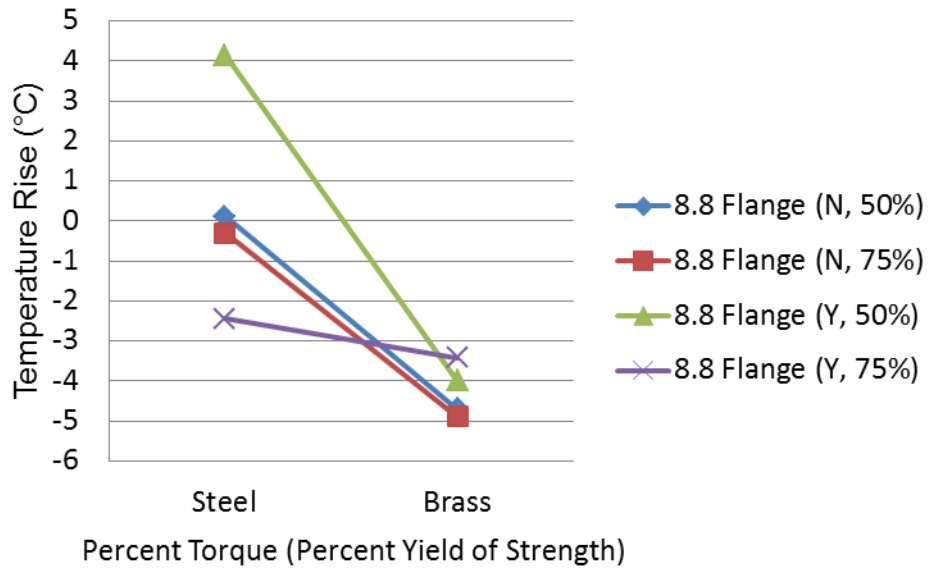

Figure 4.15: Effect of brass nut

In addition, boxplots of nut material (Figure 4.16) and head type (Figure 4.17) were made using SAS™. Again, these show the brass nut results had a lower temperature rise. In addition the flange and pan heads had lower temperature rises than the hex head cases.
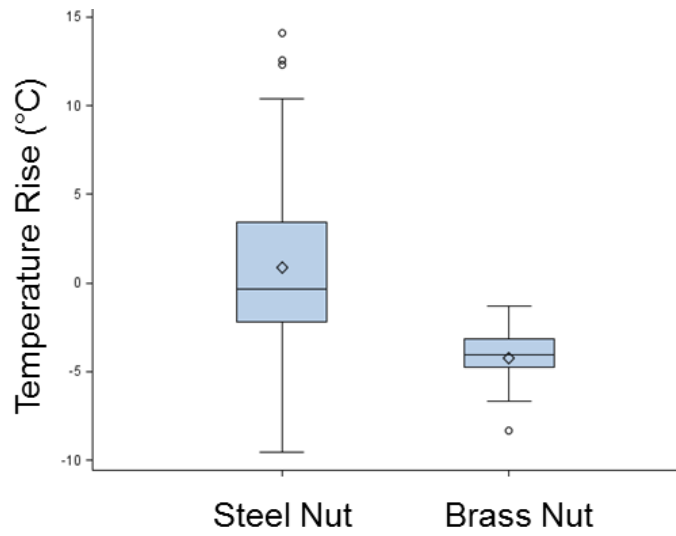
Figure 4.16: Box plot by nut material
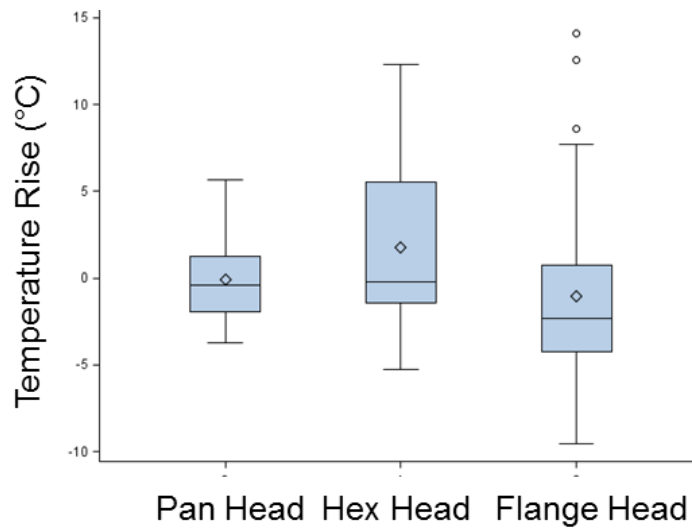
Figure 4.17: Box plot by head type

Next, a scatterplot of roughness and temperature rise was formed, as seen in Figure 4.18. The scatterplot showed a slight positive correlation between roughness and temperature rise. Therefore when the roughness increased, the temperature rise increased.
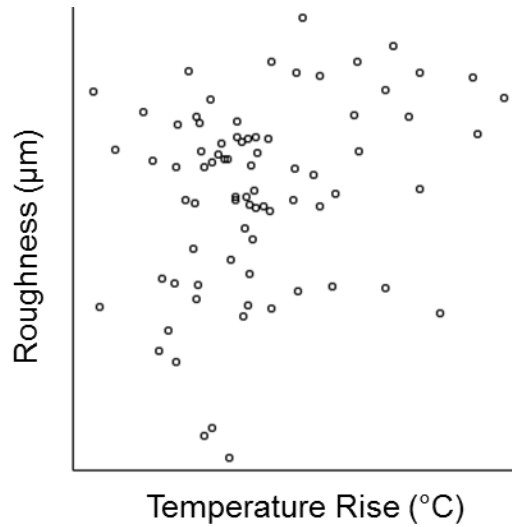
Figure 4.18: Scatterplot of 1 mm copper busbars, temperature rise

Next, forward selection, backward elimination, and stepwise regression were performed. The results are shown in Table 4.4. Each variable selection method concluded that the roughness and nut material are significant.

Table 4.4: Temperature rise, 1 mm copper busbars

Variable	Full (°C/variable unit)	Forward/Backward/Stepwise (°C/variable unit)
Intercept	-9.60 (5.74)	-6.96 (2.64)
Nut	8.74 (6.57)	-
Class – 4.8	-3.93 (10.36)	-
Class – 8.8	0.28 (1.63)	-
Class – 10.9	0 (-)	-
Head - Pan	0 (-)	-
Head - Hex	-1.88 (7.38)	-

Head - Flange	0 (-)	-
Washer	0.14 (1.02)	-
Torque	-0.04 (0.23)	-
Roughness	5.13 (2.25)	4.00 (1.33)
Roughness*Nut	-6.92 (3.28)	-2.77 (0.69)
Roughness*Head – Pan	1.68 (5.09)	-
Roughness*Head – Hex	1.97 (3.73)	-
Roughness*Head - Flange	0 (-)	-

* - data was significant in full model; values are parameter estimate (standard error)

4.5.2 Resistance Rise Analysis

The process for resistance rise analysis was repeated from the temperature rise analysis. Once again the raw data is analyzed in Figures 4.19, 4.20 and 4.21. Analyzing the raw data, the brass nut appears to reduce the response.
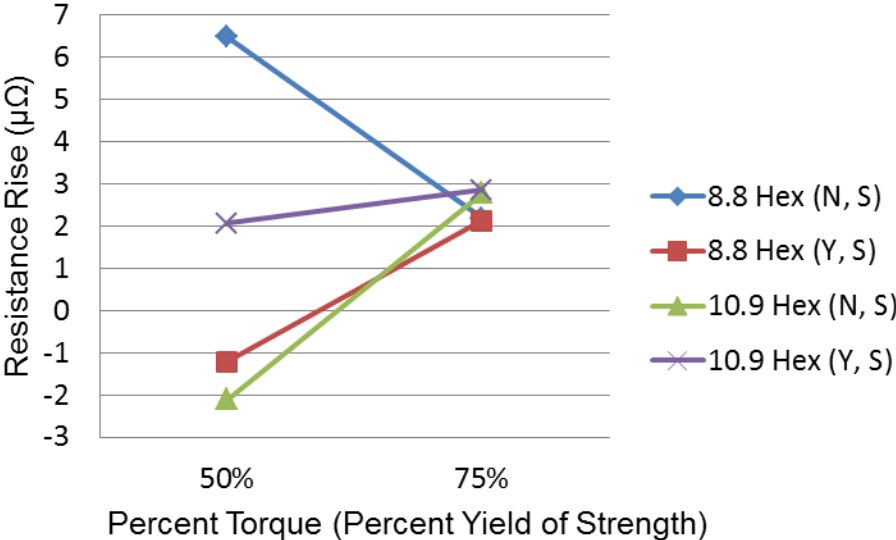
Figure 4.19: Torque graph of hex head 1 mm copper busbars
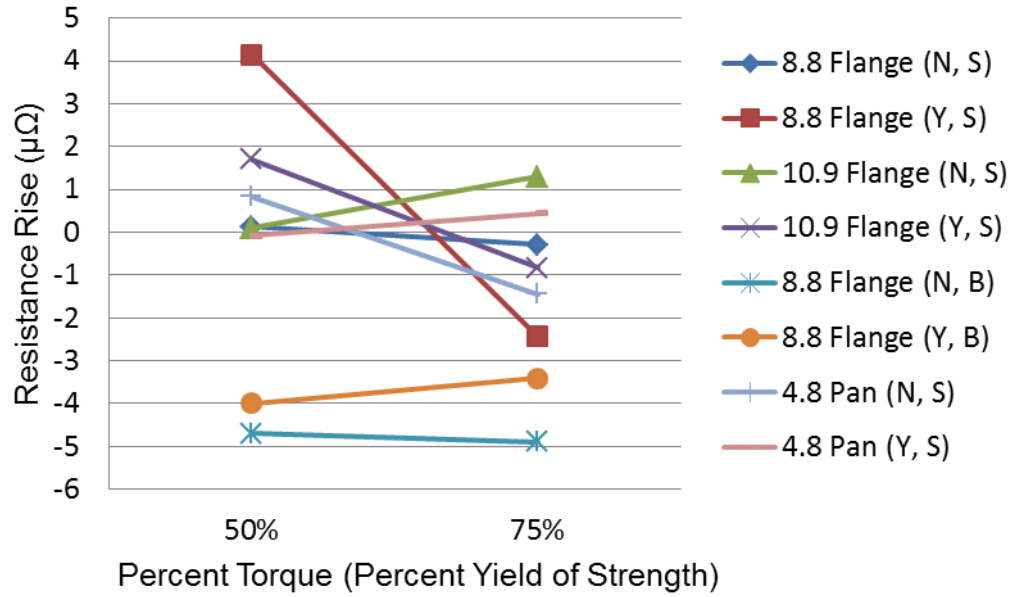
Figure 4.20: Torque graph of flange and pan head 1 mm copper busbars
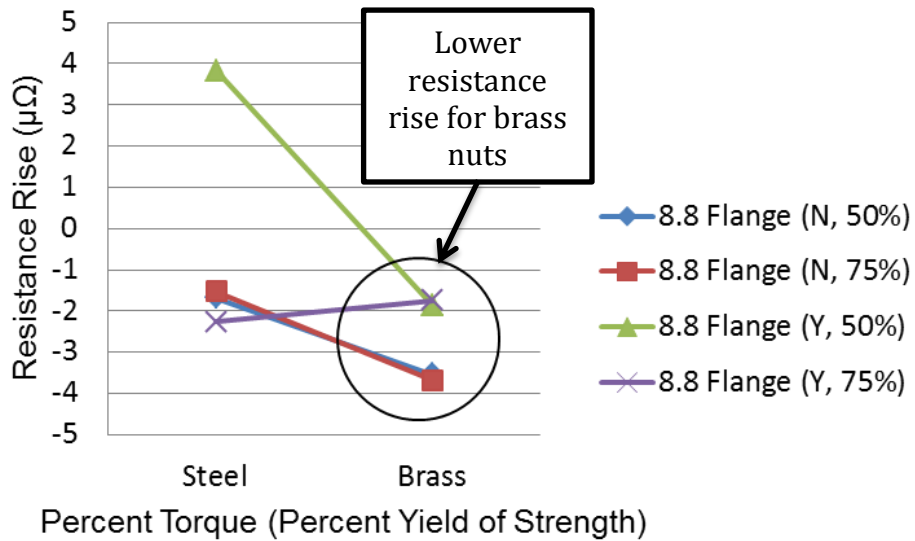

Figure 4.21: Effect of brass nut

In addition, boxplots of nut material (Figure 4.22) and head type (Figure 4.23) were made using SAS™. Again, these show the brass nut results had a lower temperature rise. In addition the flange and pan heads had lower resistance rises than the hex head cases.
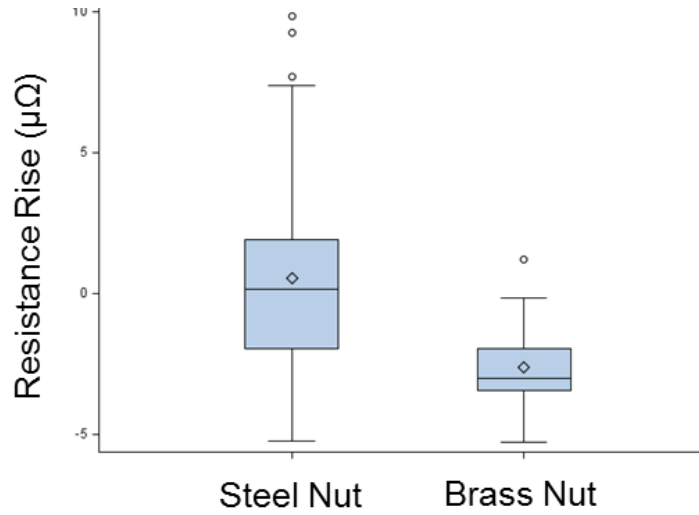

Figure 4.22: Box plot by nut material
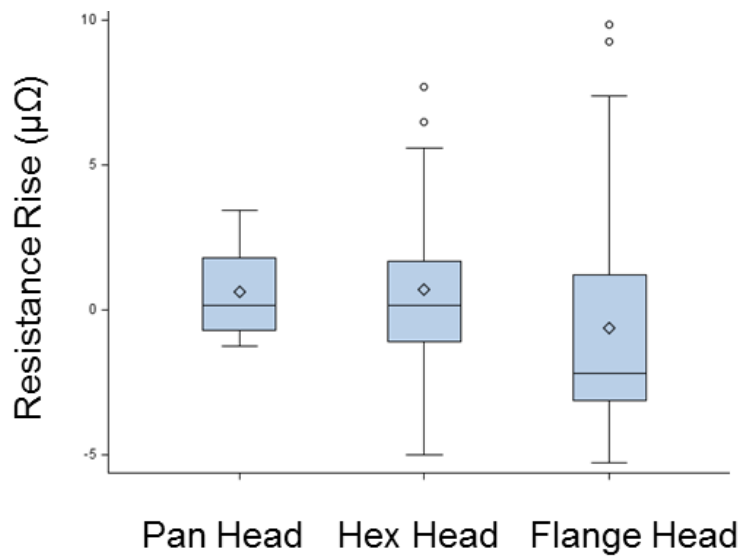
Figure 4.23: Box plot by head type

A scatterplot of roughness and resistance rise was formed, as seen in Figure 4.24. The scatterplot showed a slight positive correlation between roughness and resistance rise. Therefore when the roughness increased, the resistance rise increased.
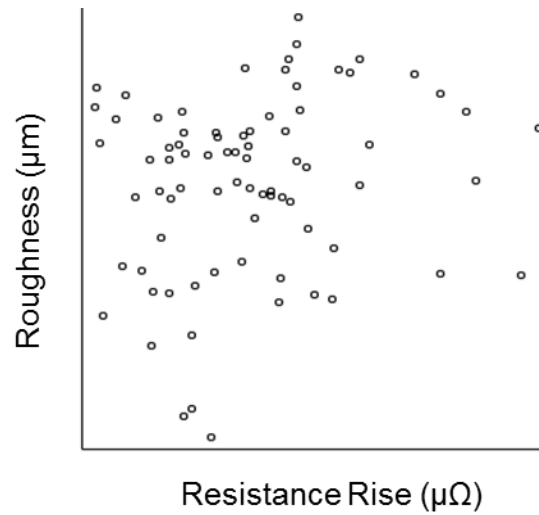
Figure 4.24: Scatterplot of 1 mm copper busbars, resistance rise

Next, forward selection, backward elimination, and stepwise regression were performed. The results are shown in Table 4.5. Each variable selection method concluded that the roughness and nut material combination term are significant.

Table 4.5: Resistance rise, 1 mm copper busbars

| Variable	Full (μΩ/variable unit)	Forward/Backward/Stepwise (μΩ/variable unit)
Intercept	1.00 (1.68)	2.93 (0.16)
Nut	1.96 (1.93)	-
Class – 4.8	1.32 (3.04)	-
Class – 8.8	-0.40 (0.48)	-
Class – 10.9	0 (-)	-
Head - Pan	0 (-)	-
Head - Hex	-0.31 (2.16)	-
Head - Flange	0 (-)	-
Washer	0.28 (0.30)	-
Torque	-0.01 (0.07)	-
Roughness	0.97 (0.66)	-
Roughness*Nut	-1.54 (0.96)	-0.74 (0.20)
Roughness*Head – Pan	-0.61 (1.49)	-
Roughness*Head – Hex	0.37 (1.09)	-
Roughness*Head - Flange	0 (-)	-

* - data was significant in full model; values are parameter estimate (standard error)

4.6 Analysis of 6 mm Aluminum Busbars

All of the assumptions were satisfied for the 6 mm aluminum busbars and no transformations were necessary. The temperature rise was for the test was defined as the

difference in the average of the last 50 maximum values and the average of the first 50 maximum values.

$$Temperature\ Rise\ =\ Average\ T_{max,\ 2nd\ half} - Average\ T_{max,\ 1st\ half}$$

The resistance rise was defined as the difference in the average electrical resistance of the second half of the test and the average electrical resistance of the first half of the test.

$$Resistance\ Rise\ =\ R_{mean,\ 2nd\ half} - R_{mean,\ 1st\ half}$$

4.6.1 Temperature Rise Analysis

First, the raw data was analyzed which could show possible relationships. Figure 4.25 shows the average relative temperature rise by case. There appears to be some correlation between torque and the response. In addition there may be a small correlation between head type and the response.
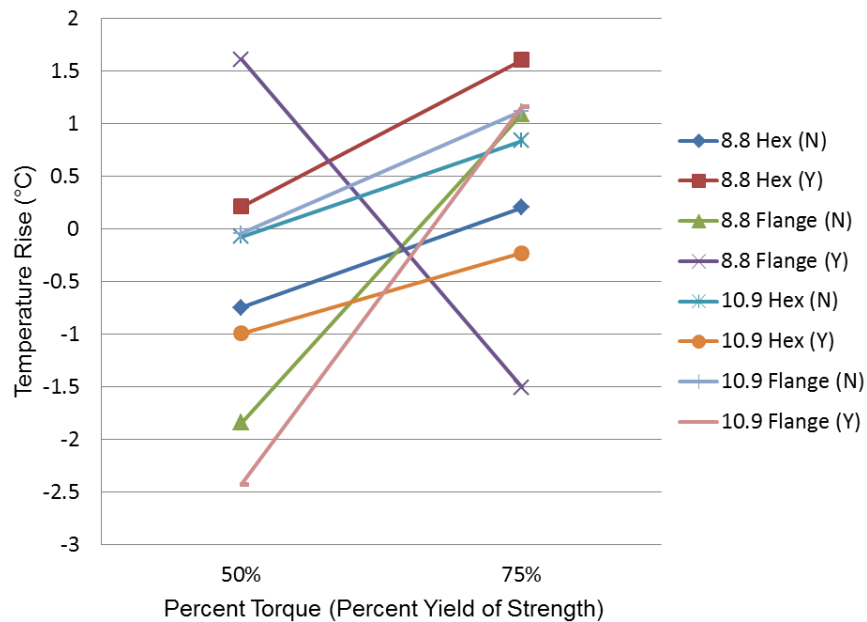

Figure 4.25: Torque graph of all 6 mm aluminum busbars

68

Again, the data is split up by head type for simplicity in Figure 4.26 and Figure 4.27. At the point the effect of torque is more obvious (see black circle).
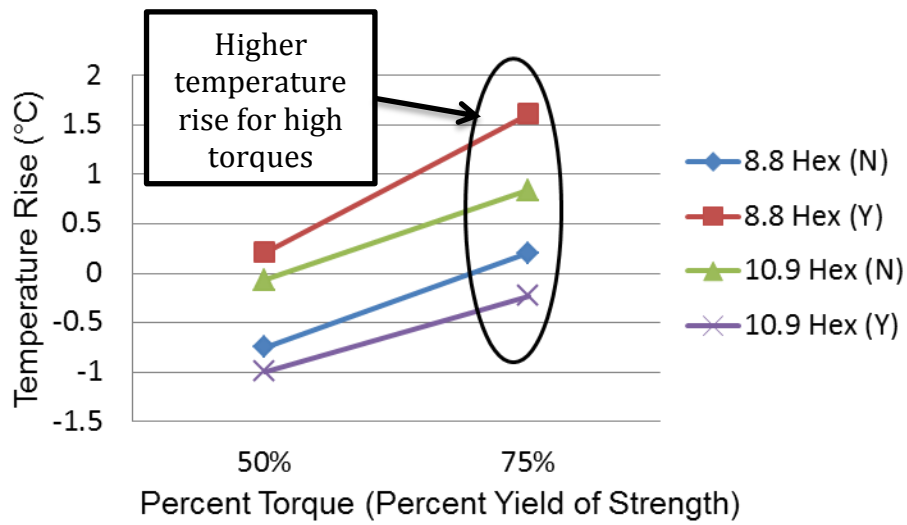
Figure 4.26: Torque graph of hex head 6 mm aluminum busbars
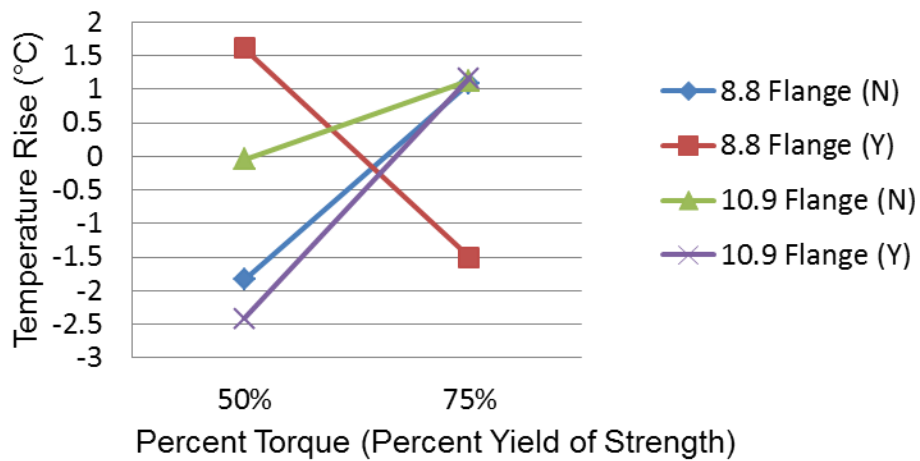
Figure 4.27: Torque graph of flange head 6 mm aluminum busbars

A scatterplot of roughness and temperature rise was formed, as seen in Figure 4.28. The scatterplot showed a slight negative correlation between roughness and temperature rise. Therefore when the roughness increased, the temperature rise decreased.
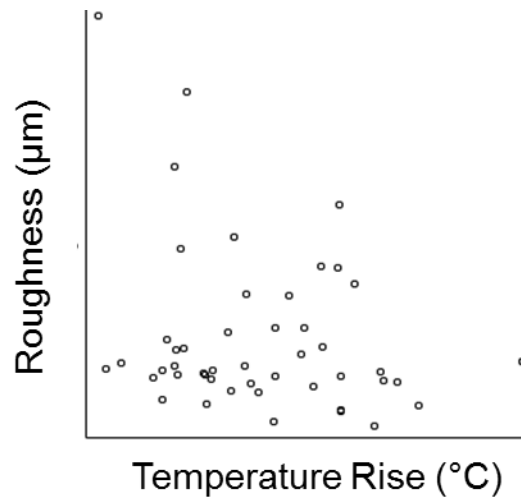
Figure 4.28: Scatterplot of 6 mm aluminum busbars, temperature rise

Next, forward selection, backward elimination, and stepwise regression were performed. The results are shown in Table 4.6. Each variable selection method concluded that roughness was the only significant variable.

Table 4.6: Temperature rise, 6 mm aluminum busbars

Variable	Full (°C/variable unit)	Forward/Backward/Stepwise (°C/variable unit)
Intercept	-2.80 (4.54)	2.57 (1.39)
Class	-2.25 (1.33)	-
Head	5.61 (4.12)	-
Washer	3.40 (5.27)	-
Torque	0.09 (0.05)	-
Roughness	-2.91 (2.08)	-2.26 (1.14)
Washer*Torque	-0.04 (0.07)	-
Washer*Roughness	-0.75 (2.53)	-
Roughness*Head	-5.11 (3.67)	-

* - data was significant in full model; values are parameter estimate (standard error)

4.6.1 Resistance Rise Analysis

The process for resistance rise analysis was repeated from the temperature rise analysis. Once again the raw data is analyzed in Figures 4.29 and 4.30. Analyzing the raw data showed little correlation between predictor and response variables.
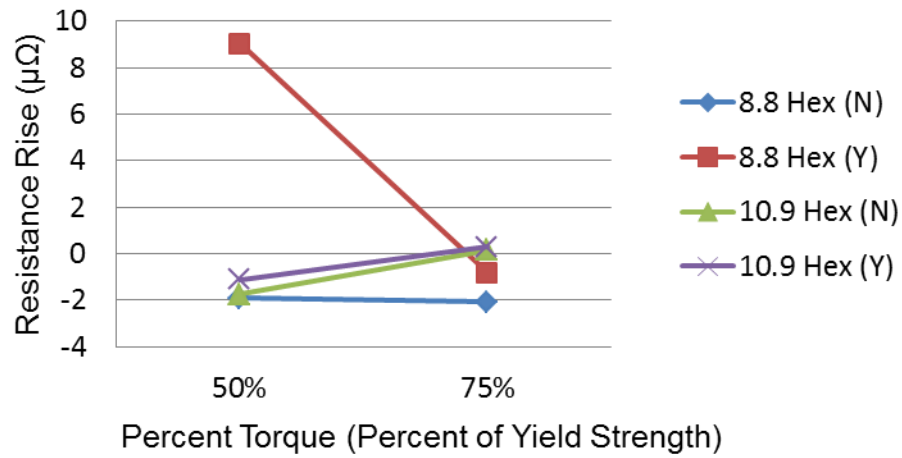
Figure 4.29: Torque graph of hex head 6 mm aluminum busbars
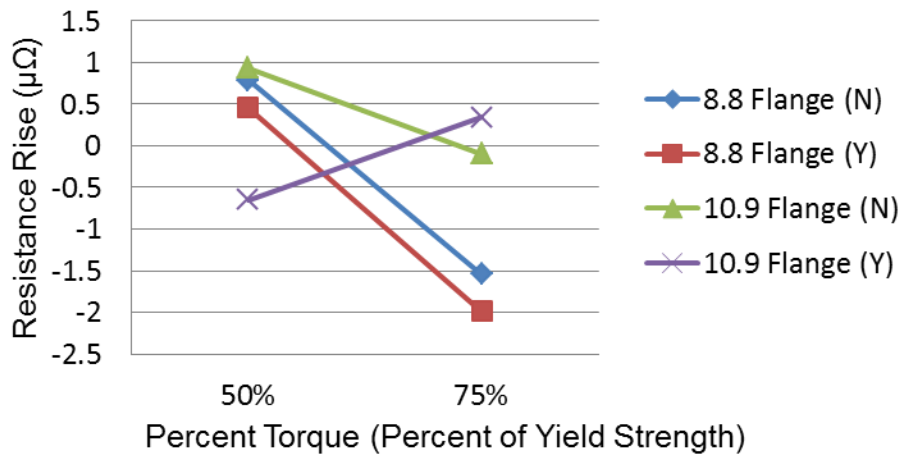
Figure 4.30: Torque graph of flange head 6 mm aluminum busbars

A scatterplot of roughness and temperature rise was formed, as seen in Figure 4.31. The scatterplot showed a slight negative correlation between roughness and resistance rise. Therefore when the roughness increased, the resistance rise decreased.
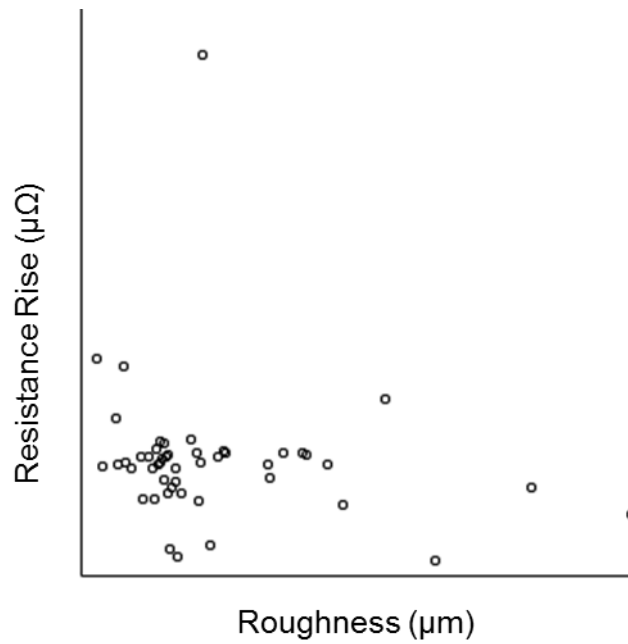
Figure 4.31: Scatterplot of 6 mm aluminum busbars, resistance rise

Next, forward selection, backward elimination, and stepwise regression were performed. The results are shown in Table 4.7. Forward selection and stepwise regression concluded roughness was significant, while backward elimination showed the combination terms of washer and torque, along with washer and roughness, were significant.

Table 4.7: Resistance rise, 6 mm aluminum busbars

Variable	Full (µΩ/variable unit)	Forward /Stepwise (µΩ/variable unit)	Backward (µΩ/variable unit)
Intercept	-0.35 (3.71)	7.49 (1.11)	5.46 (0.51)
Class	0.03 (1.09)	-	-
Head	0.12 (3.40)	-	-
Washer	2.21 (4.38)	-	-
Torque	0.01 (0.04)	-	-
Roughness	-0.21 (1.71)	-1.83 (0.92)	-
Washer*Torque	0.02 (0.06)	-	0.04 (0.02)
Washer*Roughness	-2.94 (2.07)	-	-2.47 (1.07)
Roughness*Head	0.83 (3.04)	-	-

* - data was significant in full model; values are parameter estimate (standard error)

Chapter 5

Conclusions and Future Work

A test stand was built to study the behavior of bolted joints when cycling high DC current up to 100 times. Sixty different material combinations (provided by the sponsor) were tested. Temperature and voltage readings were taken during the test as a way to determine joint reliability. At the end of testing a statistical analysis was performed on each of the different busbar types to determine which combination of parts played a significant role in determining a bolted joint's reliability. The variables that proved statistically significant, along with their effect, are listed in Table 5.1

Table 5.1 shows which variables were significant for each response of each bar type. It then notes what the effect of that variable has. For example, the significant variable for temperature rise of 6 mm aluminum busbars was roughness. The correlation was 'decreases'. Therefore a bolted joint with higher roughness will have a lower resistance rise (and better reliability). Thus, from observing the table it can be concluded which variables are beneficial to use in a bolted joint.

Table 5.1: Significant variables and their correlations

Busbar Type	Response Variable	Significant Variables (I = Interaction, S = Standalone, IS = Both)	Variable that results in best performance
6 mm Copper	Temperature Rise	Roughness (IS)	Higher/Lower Roughness
		Head (IS)	Flange Head
	Resistance Rise	Torque (I)	High Torque
1 mm Copper	Temperature Rise	Roughness (IS)	Lower Roughness
		Nut (I)	Brass Nut
	Resistance Rise	Roughness (I)	Lower Roughness
		Nut (I)	Brass Nut
6 mm Aluminum	Temperature Rise	Roughness (I)	Higher Roughness
	Resistance Rise	Roughness (IS), with washer	High Roughness
		Washer (I), with Torque and Roughness	Belleville Washer Present
		Torque (I), with Washer	Lower Torque

The common result amongst all busbar types was that roughness is statistically significant. In some cases, such as the 6 mm aluminum busbars, a higher roughness will increase the number of a-spots, as discussed in Chapter 2. Additional a-spots will then decrease the electrical resistance because there will be more paths for current to flow. Furthermore, a lower resistance will result in a lower temperature rise, thus improving reliability.

In other cases, such as the 1 mm copper busbars, a higher roughness increased the electrical resistance and temperature rise. If the roughness were increased too much, the surface area of the contacts would decrease because of the asperity size. Hence, because of the different correlations between roughness and the responses, the roughness of the different busbars was compared, as see in Figure 5.1. The average roughness of all the busbar joints is displayed. The 1 mm copper busbars have a higher roughness than the 6 mm aluminum busbars. Therefore, since a lower roughness provided a lower response for the 1 mm copper busbars and a higher roughness provided a lower response for the 6 mm aluminum busbars, it was concluded by the author that there would be some optimum roughness which occurred between the averages of the 1 mm copper busbar average roughness and the 6 mm aluminum busbar average. This value was approximately 1.5 μm.
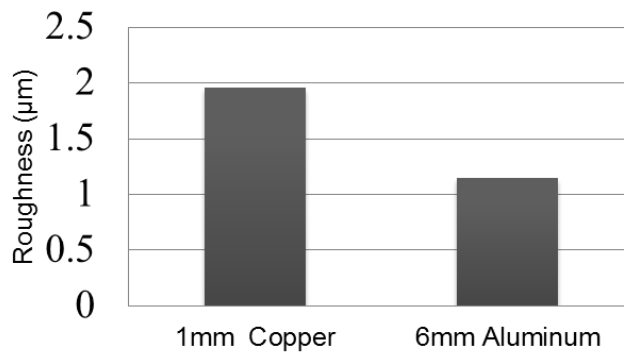

Figure 5.1: Roughness by busbar type

5.1　6 mm Copper Busbar Conclusions

The significant variable for the temperature rise response was an interaction term that consisted of roughness and head type. This interaction term is reasonable because separately, the two terms can result in a lower electrical resistance according to literature. An increase in roughness affects the size and number of a-spots [8] and can reduce the resistance [9]. The use of the flange head relative to the hex head will also increases the number of conducting paths by distributing high pressures over a larger area contact area. Thus, more a-spots will form further away from the bolt head. Hence, it is reasonable to expect the number of conducting paths to increase if the roughness is increased and a flange bolt head is used.

The significant variable for resistance rise was torque. A higher torque will allow increase the compression force of the busbars. This will result in more asperities making (better) contact resulting in more a-spots. More a-spots will result in the joint having a lower resistance rise.

5.2　1 mm Copper Busbar Conclusions

The significant variables of the temperature rise response was a combination term consisting of roughness and the nut material, along with the roughness as a single term. A higher roughness resulted in higher temperature rise, as discussed earlier in this chapter. However, the combination term had a negative correlation with the response. Therefore it was concluded that the use of the brass nut improved performance. However this benefits of the brass nut were more prevalent when the roughness was lower.

The significant varialbe of the resistance rise was a combination term consisting of roughness and nut material. Both terms can decrease the resistance rise individually. However that affect could be amplified when the variables are combined.

5.3   6 mm Aluminum Busbar Conclusions

The only variable which proved significant in the temperature rise was roughness. As discussed previously it is logical for an increase in roughness to decrease resistance rise and temperature rise.

The significant variables of resistance rise were roughness, and a combination term consisting of the presence of a washer and roughness, and a combination term consisting of washer and torque. As discussed previously, an increase in roughness can increase the number of a-spots and reduce the contact resistance. A washer can improve the performance through increasing the pressure distribution. In addition, a Belleville washer will counter the deviations in force due to dissimilarities in thermal expansion between the steel bolts and aluminum busbars. It is logical that the washer term is significant for the aluminum busbar type but none of the copper busbar types since the aluminum busbars have a larger thermal expansion coefficient than copper busbars. Therefore the dissimilirities in thermal expansion between the busbars and bolt will be larger and the washer would be more beneficial than if the bolt and busbar thermal expansions were more similar. Therefore the combination of a higher roughness and Belleville washer would results in a lower resistance rise. However, the combination of the washer variable and torque resulted in a higher response. It is concluded that the higher torque will cause higher stress when the parts thermally expand. The higher torque makes the joint more

mechanically rigid. Hence, when the (relatively high) thermal expansion of the aluminum busbars takes place, the bolt will deform more, harming the resilience of the contact.

5.4   Future Work

An experiment was designed to test material combinations of bolted joints. Afterwards a statistical analysis was performed on the data. The experience of this project improved insight on ways to possibly advance this research. Examples of future work are broken up into experimental proposals followed afterwards by statistics proposals presented.

First, many experiments in the literature review took force measurements of the bolt in addition to temperature and voltage drop measurements. The compressive force of the joint was shown to be very helpful in determining the wellbeing of the joint.

Second, the expansion of the fastener could be measured by taking caliper readings of the fastener length before and after each test. This measurement would be helpful in monitoring how much the fastener relaxes during cycling. However, to get accurate results the ends of the fastener would need to be machined prior to testing. If several test runs (such as in this work) were to take place, the extra machining required would add a large amount of preparation time.

Third, different washer combinations have been tested in literature. Rather than using a single, Belleville washer, a different combination of different types of washers could be used.

Fourth, in the present experiment the roughness was obtained by using a stylus profilometer. Alternatively, the roughness could be obtained using an optical profilometer. In addition, the surface could be finished to control the friction. It could then be tested which roughness value was optimal.

Fifth, several cases (60) were tested in this research. In the future work, the number of predictor variables could be narrowed down so that more data could be gathered on fewer predictor variables. This would potentially create better statistical results. Additionally, it would be beneficial if there were fewer categorical variables and more continuous variables. The relatively large number of categorical variables made it difficult to obtain a good fit on the data. A higher coefficient of determination (R^2) could be achieved by doing this.

Statistically, analysis like multivariate linear regression could performed on the gathered data. For example, a nonlinear fit could be experimented with. In addition, multivariate linear regression analysis could be performed on the data. Multivariate linear regression analyzes all response variables simultaneously. Therefore, if the response variables have an effect on each other (in this case they do), then a higher coefficient of determination (R^2) could possibly be achieved through capturing this effect.

References

1. Braunovic, M., *Effect of connection design on the contact resistance of high power overlapping bolted joints.* Components and Packaging Technologies, IEEE Transactions on, 2002. **25**(4): p. 642-650.

2. Braunovic, M. and M. Marjanov, *Thermoelastic ratcheting effect in bolted aluminum-to-aluminum connections.* Components, Hybrids, and Manufacturing Technology, IEEE Transactions on, 1988. **11**(1): p. 54-63.

3. Harris, F.W., *Electrical Contact Resistance.* Electric Journal, 1913. **10**: p. 637.

4. Holm, R. and E. Holm, *Electric contacts handbook.* 3rd ed1958, Berlin: Springer.

5. Braunovic, M. *Evaluation of different platings for aluminum-to-copper connections*. in *Electrical Contacts, 1991. Proceedings of the Thirty-Seventh IEEE Holm Conference on*. 1991.

6. Williamson, J.B.P., *Recent Studies on the Physics of Electrical Connector Surfaces.* Parts, Materials and Packaging, IEEE Transactions on, 1966. **2**(3): p. 71-75.

7. Melsom, S.W. and H.C. Booth, *The efficiency of overlapping joints in copper and aluminium busbar conductors.* Electrical Engineers, Journal of the Institution of, 1922. **60**(312): p. 889-899.

8. Bailey, J.C., *Bolted connections in aluminium busbar.* The Engineer, 1955: p. 551-554.

9. Naybour, R.D. and T. Farrell, *Degradation mechanisms of mechanical connectors on aluminium conductors.* Electrical Engineers, Proceedings of the Institution of, 1973. **120**(2): p. 273-280.

10. Braunovic, M., *Effect of Contact Aid Compounds on the Performance of Bolted Aluminum-to-Aluminum Joints Under Current Cycling Conditions.* Components, Hybrids, and Manufacturing Technology, IEEE Transactions on, 1986. **9**(1): p. 59-70.

11. Jackson, R.L., *Significance of surface preparation for bolted aluminium joints.* Generation, Transmission and Distribution, IEE Proceedings C, 1981. **128**(2): p. 45-54.

12. Braunovic, M., *Effect of Current Cycling on Contact Resistance, Force, and Temperature of Bolted Aluminium-to-Aluminium Connectors of High Ampacity.* Components, Hybrids, and Manufacturing Technology, IEEE Transactions on, 1981. **4**(1): p. 57-69.

13. Tzeneva, R., Y. Slavtchev, N. Mastorakis, and V. Mladenov, *New Design of Aluminum Bolted Busbar Connections*, in *13th WSEAS International Conference on CIRCUITS*2009: Hersonissos, Crete Island, Greece.

14. Schoft, S., H. Lobl, J. Kindersberger, and S. Grossmann, *Creep Ageing of Bolted Electrical Busbar Joints*, in *19th International Conference on Electric Contact Phenomena*1998: Nuremberg. p. 269-273.

15. Schoft, S. *Joint resistance depending on joint force of high current aluminum joints*. in *Electrical Contacts, 2004. Proceedings of the 50th IEEE Holm Conference on Electrical Contacts and the 22nd International Conference on Electrical Contacts*. 2004.

16. Xin, Z. and T. Schoepf. *Characteristics of Overheated Electrical Joints Due to Loose Connection*. in *Electrical Contacts (Holm), 2011 IEEE 57th Holm Conference on*. 2011.

17. Schoft, S., J. Kindersberger, and H. Lobl. *Joint Resistance of Busbar-Joints with Randomly Rough Surfaces*. in *21th Conference on Electrical Contacts*. 2002. Zurich.

18. Schoft, S. *Measurement and calculation of the decreasing joint force in high current aluminum joints*. in *Electrical Contacts, 2004. Proceedings of the 50th IEEE Holm*

Conference on Electrical Contacts and the 22nd International Conference on Electrical Contacts. 2004.

19. Schlegel, S., S. Grossmann, Lo, x, H. bl, M. Hoidis, U. Kaltenborn, and T. Magier. *Joint Resistance of Bolted Copper - Copper Busbar Joints Depending on Joint Force at Temperatures beyond 105 °C*. in *Electrical Contacts (HOLM), 2010 Proceedings of the 56th IEEE Holm Conference on*. 2010.

20. Bergmann, R., H. Lobl, H. Bohme, and S. Grossmann, *Model to assess the reliability of electrical joints.* Electrical Contacts, 1996: p. 180-188.

21. Farahat, M.A., E. Gockenbach, A.A. El-Alaily, and M.M. Abdel Aziz. *Effect of coating materials on the electrical performance of copper joints*. in *Electrical Contacts, 1996. Proceedings of the Forty-Second IEEE Holm Conference on Electrical Contacts. Joint with the 18th International Conference on Electrical Contacts*. 1996.

22. Braunovic, M., V. Konchits, and N. Myshkin, *Electrical Contacts: Fundamentals, Applications and Technology*2006: CRC Press.

23. Hare, T.K., *Investigation of Nickel Plated Aluminum Wire Using Analytical Electron Microscopy.* 1987.

24. Jackson, R.L., *Electrical performance of aluminium/copper bolted joints.* Generation, Transmission and Distribution, IEE Proceedings C, 1982. **129**(4): p. 177-184.

25. Braunovic, M., *FRETTING IN NI-COATED ALUMINUM CONDUCTORS.* Ieee Transactions on Components Hybrids and Manufacturing Technology, 1991. **14**(2): p. 327-336.

26. Braunovic, M., *Evaluation of Different Types of Contact Aid Components for Aluminum-to-Aluminum Connectors and Conductors.* Components, Hybrids, and Manufacturing Technology, IEEE Transactions on, 1985. **8**(3): p. 313-320.

27. Popa, I. and A.I. Dolan. *Numerical modeling of DC busbar contacts*. in *Optimization of Electrical and Electronic Equipment (OPTIM), 2012 13th International Conference on*. 2012.

28. Wileman, J., M. Choudhury, and I. Green. *Computation of member stiffness in bolted connections*. in *Proceedings of the 1990 ASME International Computers in Engineering Conference and Exposition, August 5, 1990 - August 9, 1990*. 1990. Boston, MA, USA: Publ by ASCE.

29. Budynas, R.N., J., *Mechanical Engineering Design*. 9th ed2011.

30. Polchow, J.R., S.V. Angadi, R.L. Jackson, C. Song-Yul, G.T. Flowers, L. Bong-Yi, and Z. Liang. *A Multi-Physics Finite Element Analysis of Round Pin High Power Connectors*. in *Electrical Contacts (HOLM), 2010 Proceedings of the 56th IEEE Holm Conference on*. 2010.

31. Labrecque, C., M. Braunovic, P. Terriault, F. Trochu, and M. Schetky. *Experimental and theoretical evaluation of the behavior of a shape memory alloy Belleville washer under different operating conditions*. in *Electrical Contacts, 1996. Proceedings of the Forty-Second IEEE Holm Conference on Electrical Contacts. Joint with the 18th International Conference on Electrical Contacts*. 1996.

32. Braunovic, M., *Evaluation of different contact aid compounds for aluminum-to-copper connections.* Components, Hybrids, and Manufacturing Technology, IEEE Transactions on, 1992. **15**(2): p. 216-224.

33. Ramsey, F.S., Daniel, *The Statistical Sleuth: A Course in Methods of Data Analysis*. 2 ed2002.

34.   Montgomery, D.E., P.; Vining, G., *Introduction to Linear Regression Analysis*. 4th ed2006, Hobaken, New Jersey: John Wiley & Sons, Inc. 613.
35.   *Fastenal*. Available from: https://www.fastenal.com/web/home.ex.